RESEARCH AND DEVELOPMENT IN THE FIELD OF FATIGUE AND FRACTURE - MECHANICS AT THE NATIONAL AERONAUTICAL LABORATORY

K.N. Raju and R. Sunder

Materials Science Division
National Aeronautical Laboratory
Bangalore 560017

ABSTRACT

Research and development in the area of fatigue and fracture mechanics at the National Aeronautical Laboratory is described, highlighting some of the interesting and useful results obtained. The beginning of research and development activities at the National Aeronautical Laboratory dates back to late sixties. Thus what is described in this paper covers work over a period of more than a decade.

INTRODUCTION

Research and development activities at the National Aeronautical Laboratory, from the very beginning have progressed in two general directions namely (i) Fatigue life evaluation of military aircraft, and development of fatigue testing facilities and techniques, (ii) Analytical and experimental studies in fatigue crack growth and fracture mechanics.

Research and Development work in the area of fatigue and fracture mechanics started with the development of fatigue testing facilities such as constant amplitude fatigue testing machines, single actuator servo hydraulic fatigue testing machine with punched tape programmer etc. Experimental studies on fatigue crack growth to investigate the effects of overloads (Raju 1970) overaging and effects of heat on retardation due to overloads (Raju and co-workers 1972) marked the beginning of research in the area of fatigue at NAL (National Aeronautical Laboratory). In 1970 the Indian Air Force (IAF) indicated interest in fatigue life evaluation of the Gnat fighter aircraft which was a front line fighter in those days. Involvement in fatigue life evaluation of the Gnat marked the beginning of full scale fatigue testing and life evaluation programmes at NAL. This led to the development of a six actuator electro-hydraulic full scale fatigue testing facility with a tape addressed individual load level programmer and subsequently to the development of a hybrid computer controlled 24 actuator full scale fatigué testing facility. This facility with hybrid computer control was designed and built to cater to the future needs of Indian Air Force in respect of fatigue evaluation of fighter/trainer aircraft.

Analytical and experimental studies by and large are centred around various aspects of fatigue crack growth under constant and variable amplitude loading and fracture mechanics of thin sheet structures. Automated fatigue crack growth testing under flight spectrum loading

in computer controlled fatigue machines, fractographic technique of determination of crack opening stress, binary coded event registration on fracture surfaces, unified analytical modelling of fatigue crack growth, studies on the applicability of cycle counting techniques to fatigue crack growth prediction under random load histories, experimental studies on fatigue crack growth in constant K gradient fields under spectrum loading, analytical techniques of S.I.F. determination for cracked shells are some of the highlights of recent work at NAL. A brief description and discussion of research and development work at NAL is presented in this paper in two sections namely (I) Fatigue life evaluation programmes on fighter aircraft and development of fatigue testing facilities and techniques (II) Analytical and experimental studies in fatigue crack growth and fracture mechanics.

(I) FATIGUE LIFE EVALUATION PROGRAMMES AND DEVELOPMENT OF FATIGUE TESTING FACILITIES AND TECHNIQUES

(Progress reports - Raju 1973-82, Balakrishna 1976, Jategaonkar and co-workers 1976, Sunder and Raju 1982, Sunder 1984)

A comprehensive programme of work was taken up in 1970 on the fatigue life evaluation of the Gnat fighter aircraft in response to a requirement of the IAF. The Gnat, the smallest fighter in the world, during those days was a front line fighter of the IAF and evaluation of fatigue life of this aircraft was considered important. The programme involved fatigue testing of full size airframes of this aircraft. The programme began with an intensive effort to collect, from the operating squadrons, information on flight loads to which the aircraft were subjected to while flying different sorties. The information was obtained through flight-log sheets from the entire fleet of Gnat aircraft coupled with fatigue meter data from five aircraft. A full scale fatigue testing facility with six servo-hydraulic actuators was designed and built in the laboratory. This facility has a punched tape addressed 32 load level programmer with four choices for distribution of each load level among the actuators. Using this programmer any load history defined as a sequence of 32 load levels can be programmed and applied on the airframe.

The test load programme schedule was evolved from the 'g' spectrum (normal acceleration at c.g.) and flight parameter statistics obtained from an analysis of the flight load information collected. The load programme was on a flight-by-flight basis with load cycles arranged in two pyramidal programme blocks (L.H.L) corresponding to two reference weights of the aircraft to account for fuel consumption during a sortie. Fatigue tests were conducted on full scale airframes in the six actuator full scale fatigue facility. Fig.1 shows the Gnat airframe in the test rig undergoing fatigue test along with a typical flight load programme and the location of the loading patches on the wing. As a result of the fatigue life evaluation programme and the design modifications evolved significant life extension was achieved for the Gnat aircraft.

The results also formed valuable inputs in the design of the Ajeet, a variant of the Gnat. The Ajeet has the same geometry as the Gnat. The main difference is that the wings of the Ajeet have integral fuel tanks and hence the wing structure detail is different. Also the Ajeet is expected to operate in a role different from that of the Gnat. The results of the Gnat programme could not therefore be extrapolated to

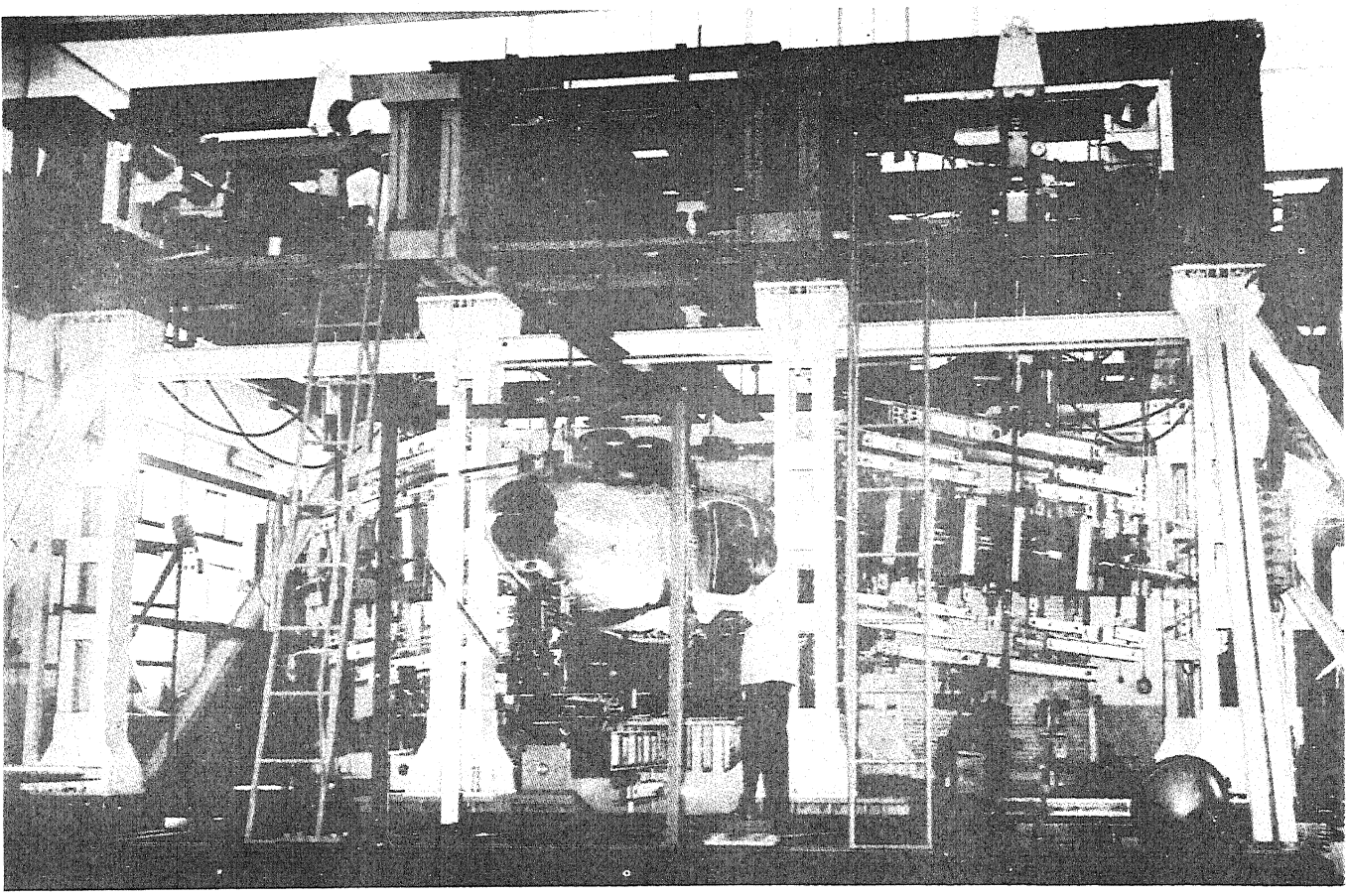

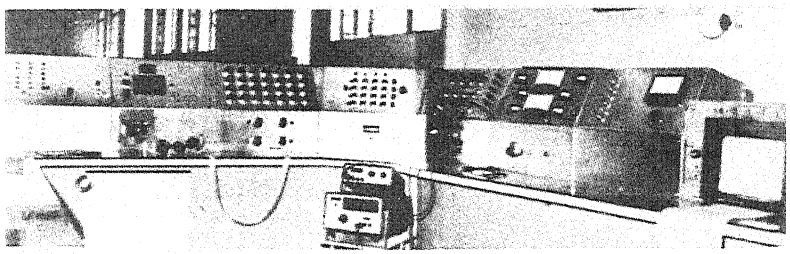

TAPE PROGRAMMER AND CONTROLLER

TIME HISTORIES OF A TYPICAL FLIGHT IN FLIGHT-BY-FLIGHT LOAD PROGRAMME APPLIED IN TEST

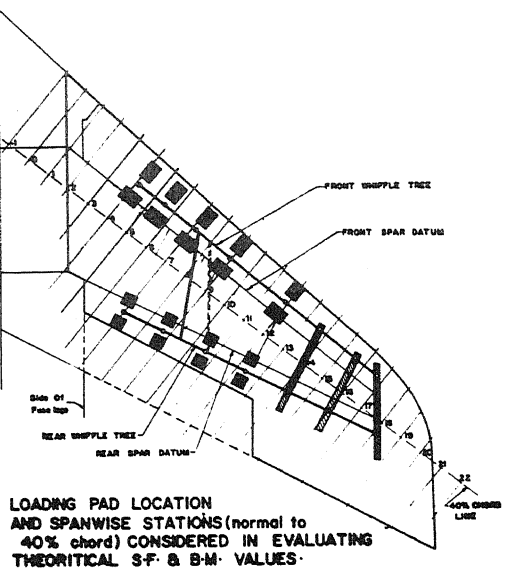

LOADING PAD LOCATION AND SPANWISE STATIONS (normal to 40% chord) CONSIDERED IN EVALUATING THEORITICAL S·F· & B·M· VALUES·

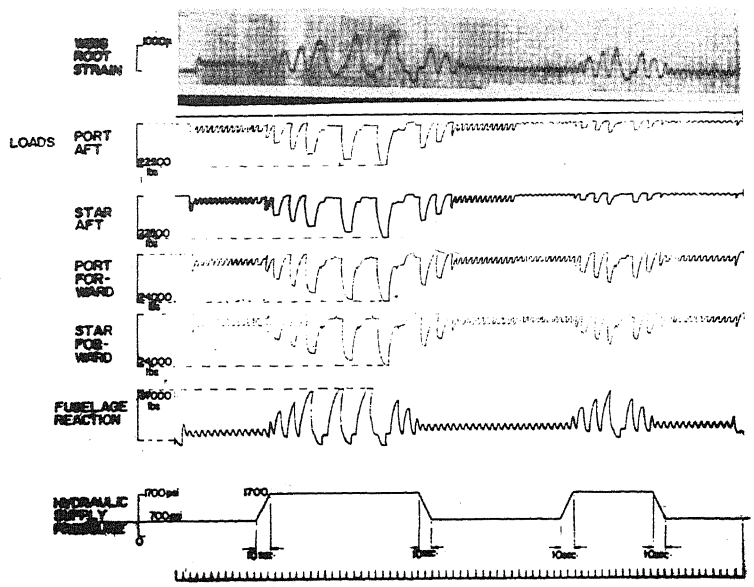

FIG 1 FATIGUE TESTING OF GNAT AIRFRAME UNDER FLIGHT-BY-FLIGHT LOAD PROGRAMME WITH L-H-L SEQUENCE OF LOAD CYCLES IN EACH FLIGHT

estimate the fatigue behaviour of the Ajeet. Hence the need arose for fatigue life evaluation programme on the Ajeet.

The Ajeet fatigue life evaluation programme was taken up and recently completed. The load programme schedule used for the full scale fatigue testing of the Ajeet airframe is again on a flight-by-flight basis, but unlike in the Gnat programme, the load sequence in each flight is random. Fuel tank and cockpit pressurisation cycles are also part of the flight-by-flight load programme schedule. Fig.2 shows the Ajeet airframe in the test rig undergoing fatigue testing. Also shown in the figure is a typical flight in the flight-by-flight load programme. The design modification evolved by HAL in the light of the test results has proved to be quite effective in significantly enhancing the fatigue life.

The limitations of the six actuator fatigue testing facility in respect of available test space and capability for simulating the variety of load distributions and load sequences the airframe experiences in service, led to the development of a 24 actuator hybrid computer controlled full scale fatigue testing facility with large test space. The facility is designed in such a manner as to enable fatigue testing of any contemporary fighter or trainer aircraft. Fig.3 shows a discarded airframe mounted in the test rig for commissioning trials with the facility. Also shown in the figure are the TDC-316 digital and AC-40 analog computers. Fig.4 and 5 show the TDC-316 configuration and the functional diagram of the complete control system. Fig.6 shows the software developed for fatigue testing any airframe in the full scale fatigue testing facility. This facility will cater to the future needs of the IAF in respect of fatigue life evaluation.

Facility for flight data analysis (Sunder and Raju 1982)
(Sunder and Raju 1982)

A major and important phase in any full scale fatigue testing programme is the process of derivation of load spectrum for the aircraft to be tested. An Aircraft Flight Data Analysis System (AFDAS) was set up to derive the 'g' load spectrum and associated flight parameter statistics for combat aircraft through an analysis of photofilm based flight data records. A schemetic of this system appears in Fig.7 along with a picture of the total system. Software was developed to digitise and analyse flight data records covering hundreds of flying hours. The process of load spectrum derivation is schematically described in Fig.8. Digitised results for a typical flight are shown in Fig.9. The 'g' load spectrum derived at the conclusion of the analysis can be used in (a) Full-scale fatigue testing of airframes (b) tests on components (c) low cycle fatigue studies on notched specimen (d) fatigue crack growth studies.

Computer controlled fatigue crack propagation testing
(Sunder 1984)

An INSTRON computer controlled servo hydraulic fatigue testing machine was installed at NAL in 1982. One of the major applications of this facility is the generation of a data base on fatigue crack growth properties of aircraft materials under constant amplitude and flight-by-flight spectrum loading conditions. Photographs of the test set up appear in

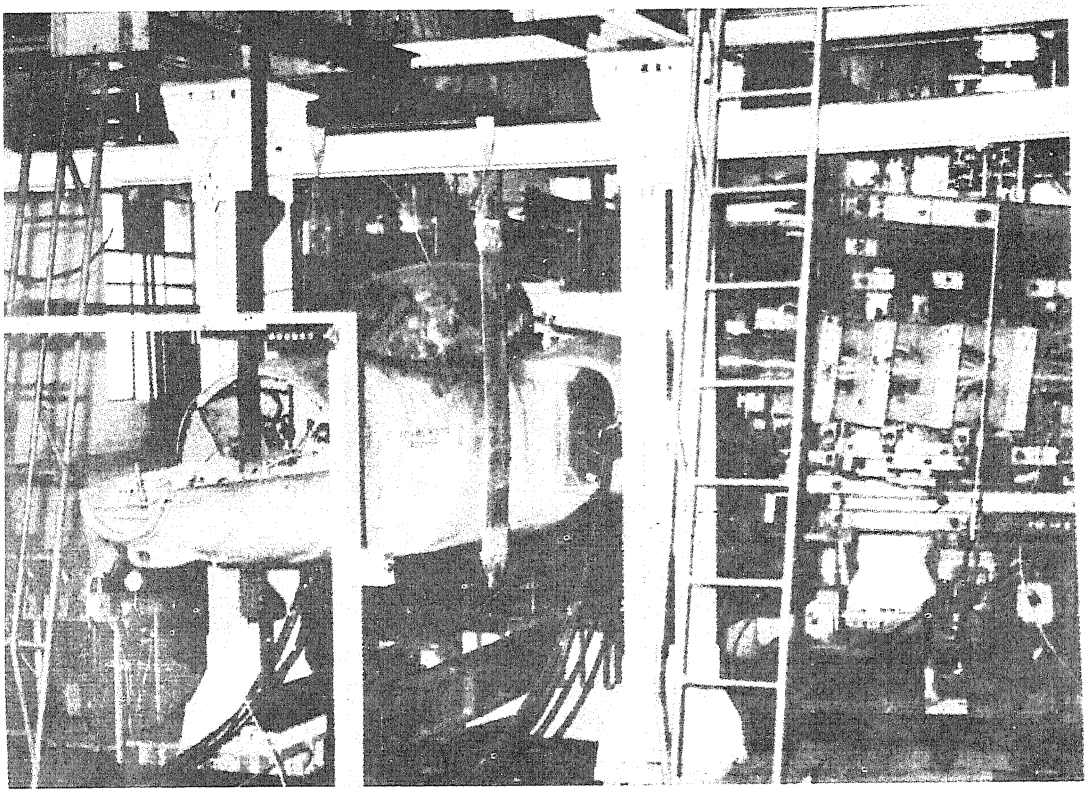

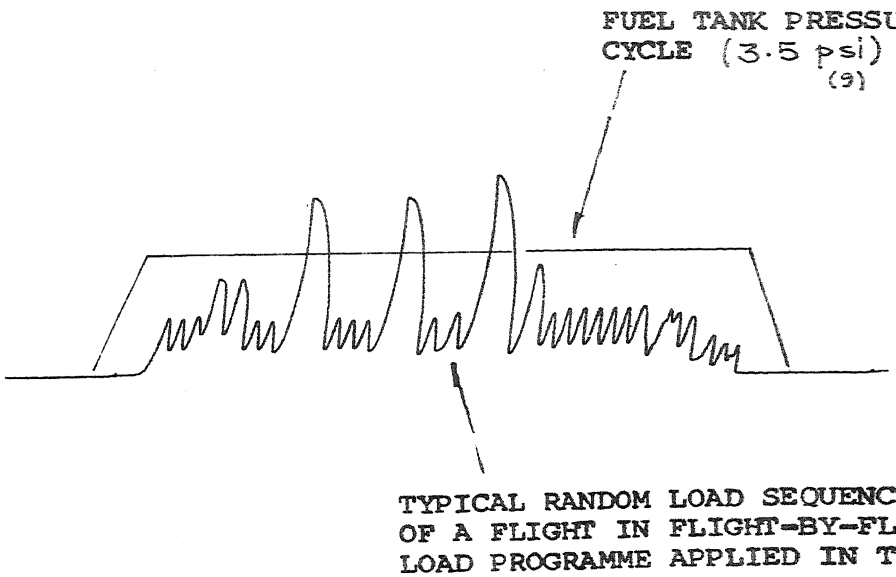

FIG 2 FATIGUE TESTING OF AJEET AIRFRAME UNDER FLIGHT-BY-FLIGHT LOAD PROGRAMME WITH RANDOM SEQUENCE OF LOAD CYCLES IN EACH FLIGHT APPLIED ALONG WITH FUEL TANK AND COCK-PIT PRESSURISATI CYCLES.

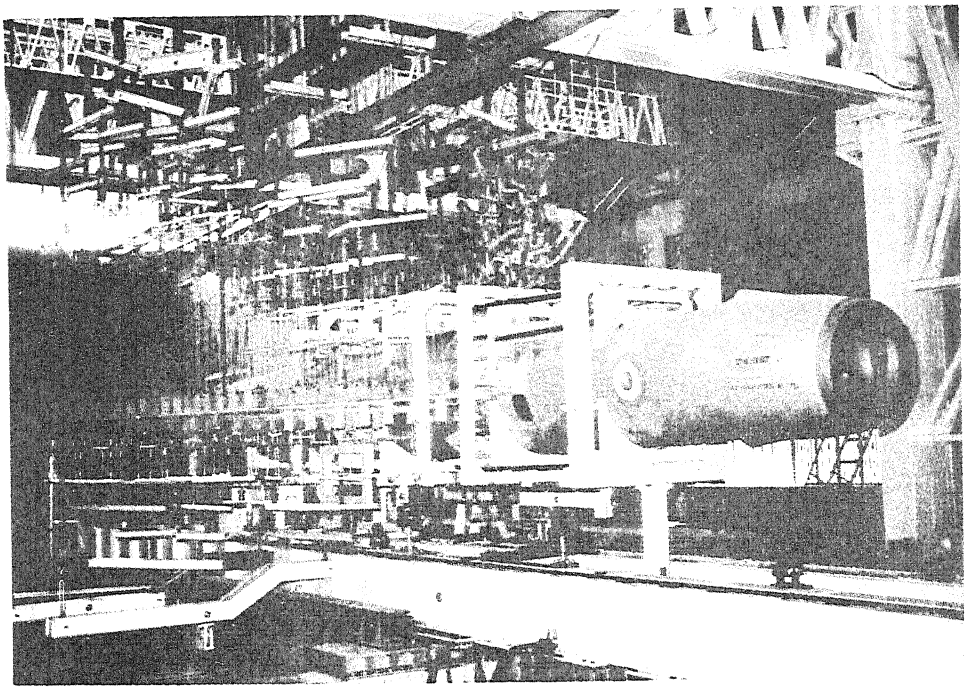

DISCARDED AIRFRAME IN TEST RIG

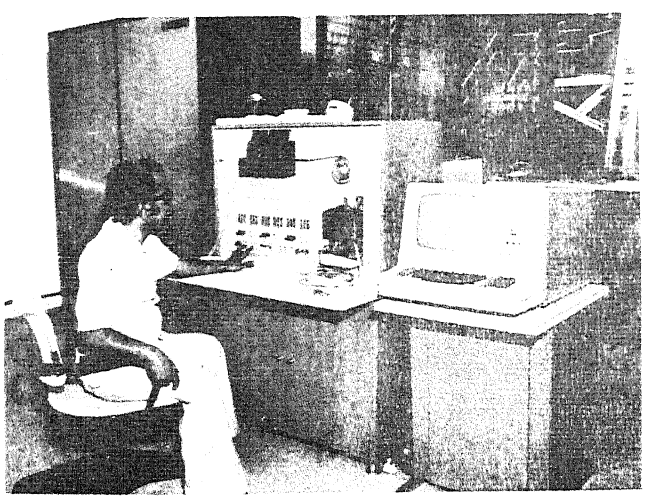

TDC-316 DIGITAL COMPUTER

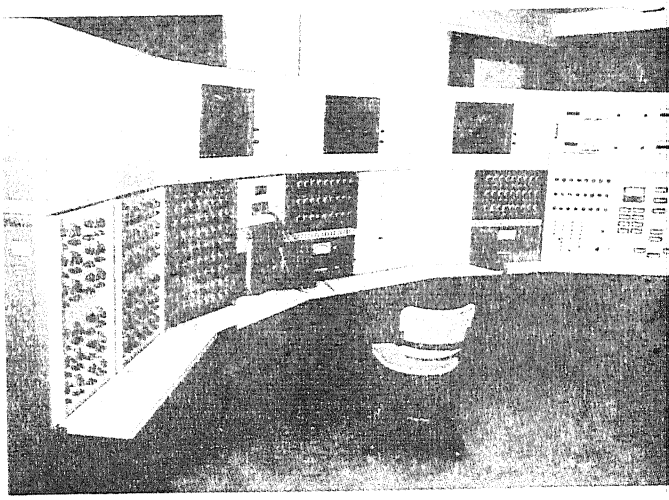

ANALOG CONTROLLER COMPLEX

FIG 3 TWENTY FOUR ACTUATOR HYBRID COMPUTER CONTROLLED FULL SCALE FATIGUE TESTING FACILITY WITH A DISCARDED AIRFRAME MOUNTED IN THE TEST RIG FOR COMMISSIONING TRIALS

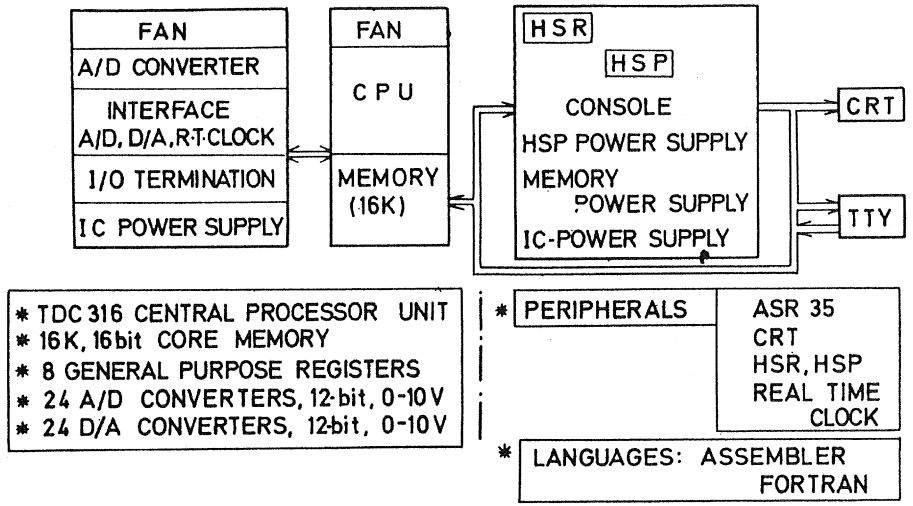

FIG 4 TDC-316 CONFIGURATION

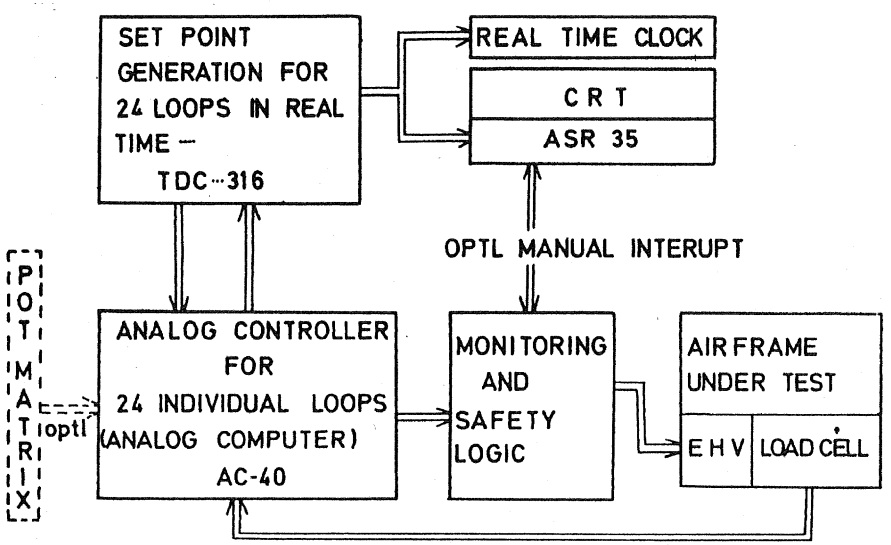

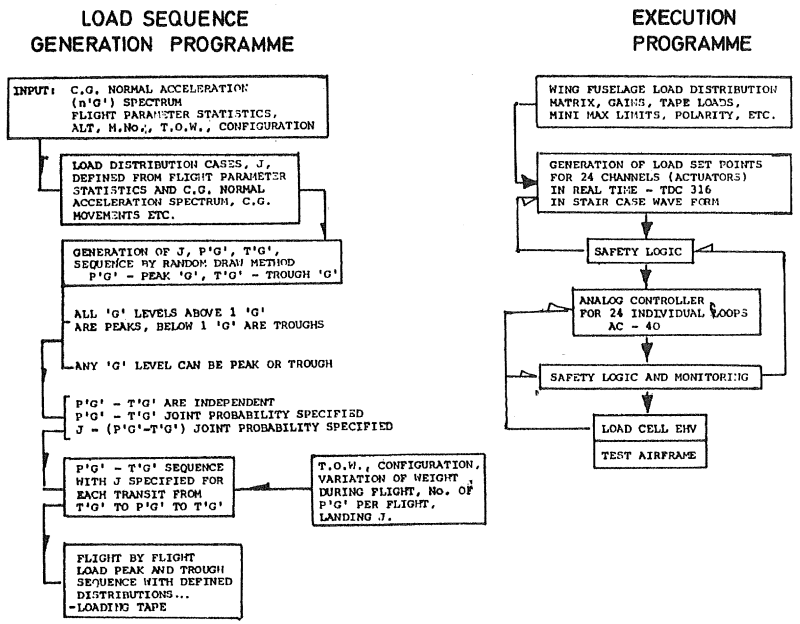

FIG 6 SOFTWARE FOR LOAD SEQUENCE GENERATION AND EXECUTION OF FULL SCALE FATIGUE TEST ON AIRFRAMES.

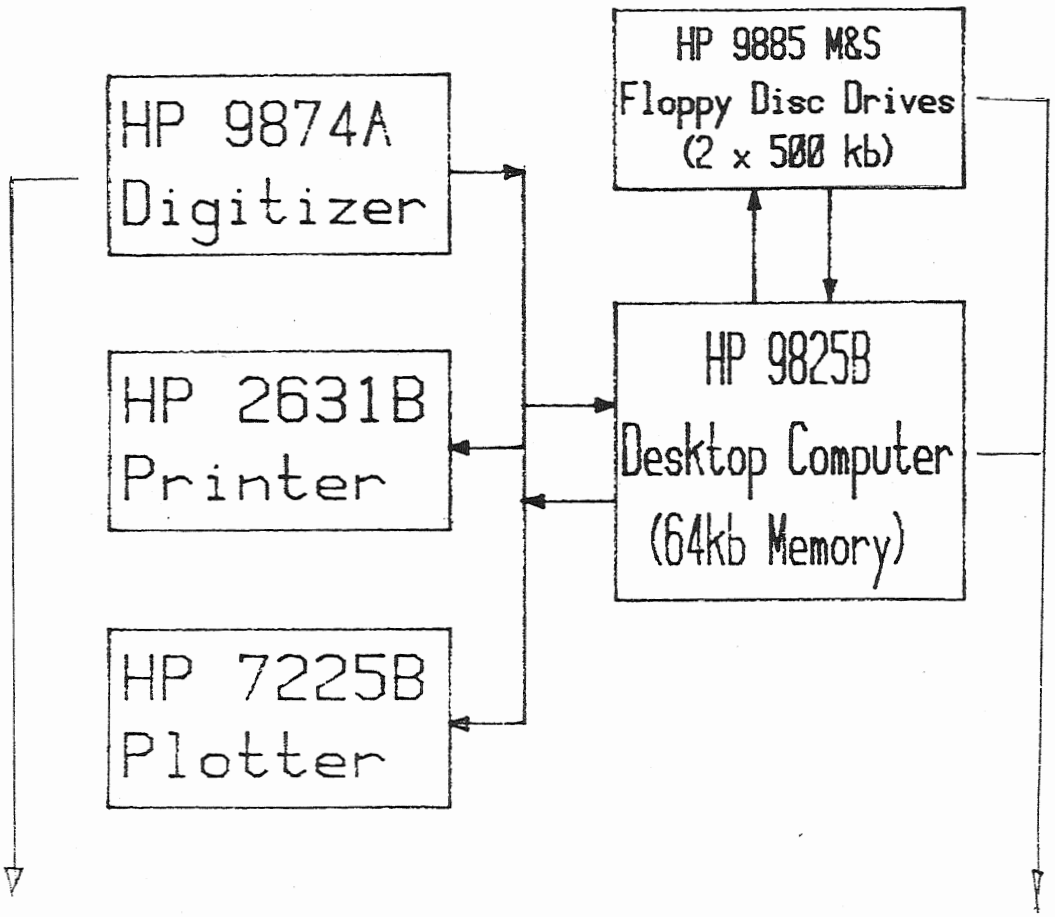

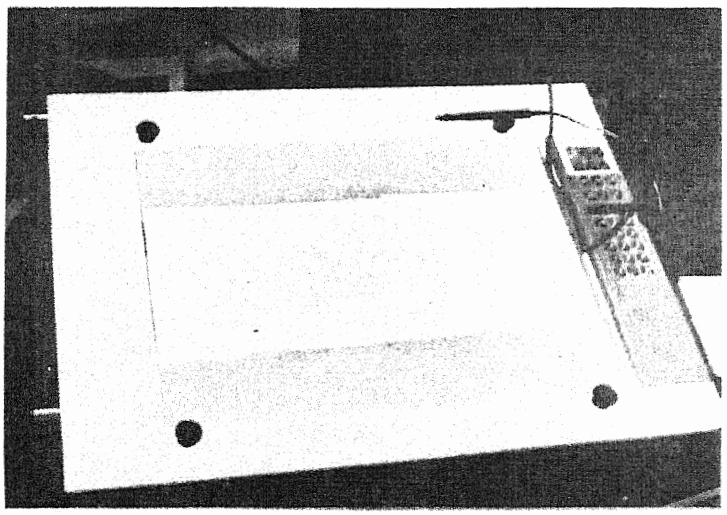

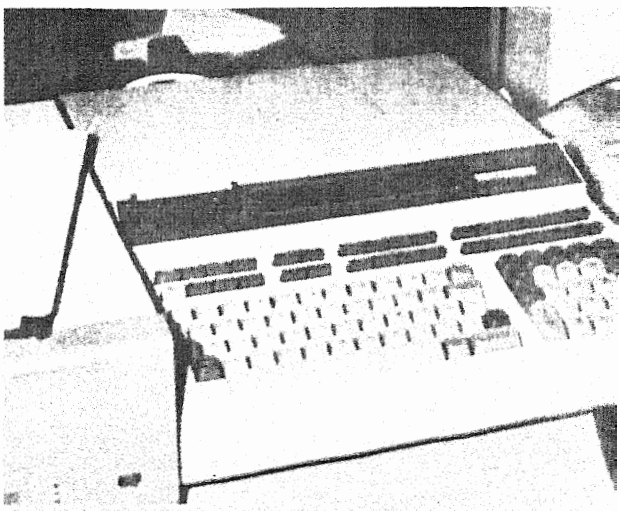

FIG 7 AIRCRAFT FLIGHT DATA ANALYSIS SYSTEM

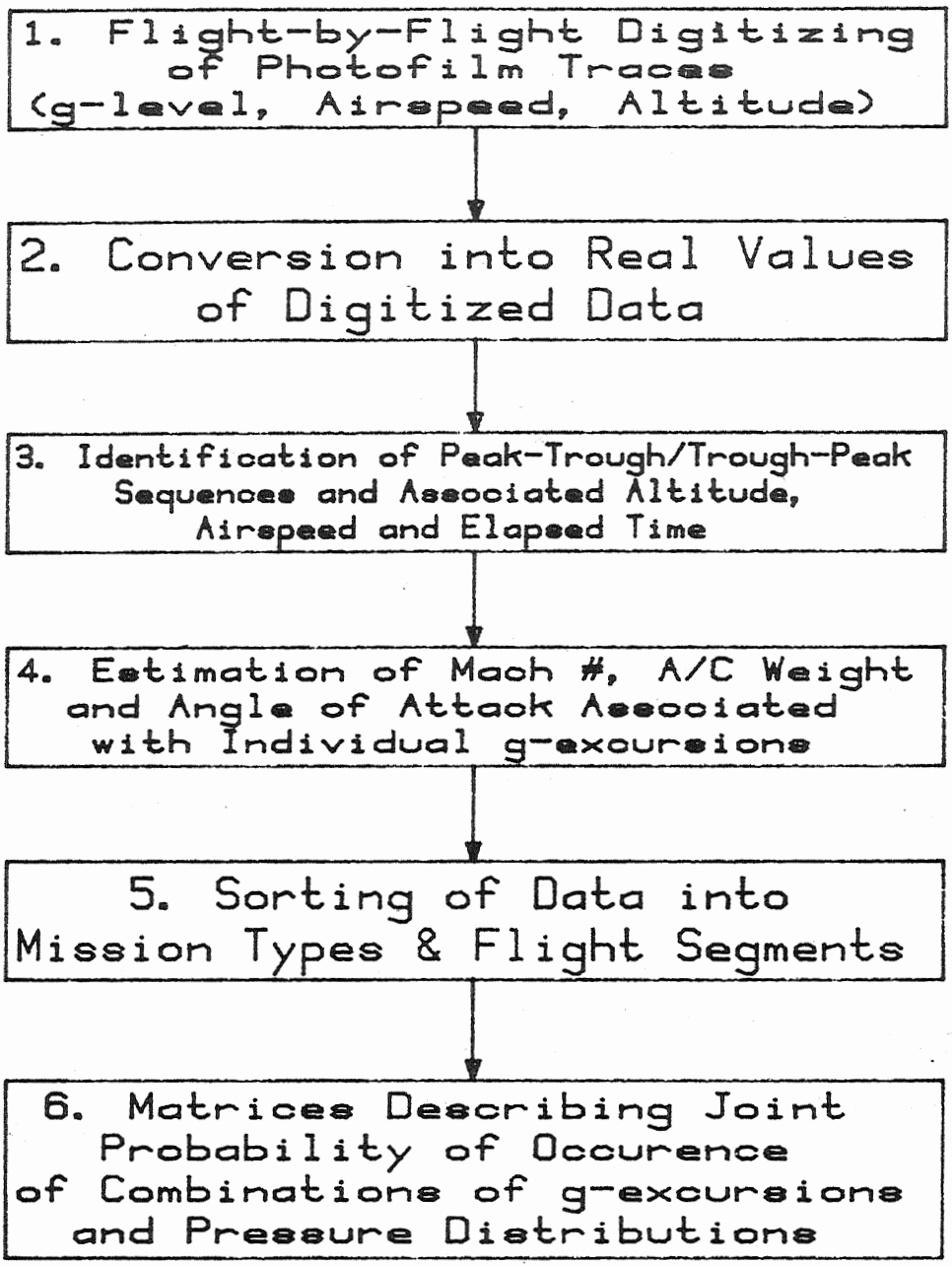

Fig. 8 Process of load spectrum derivation

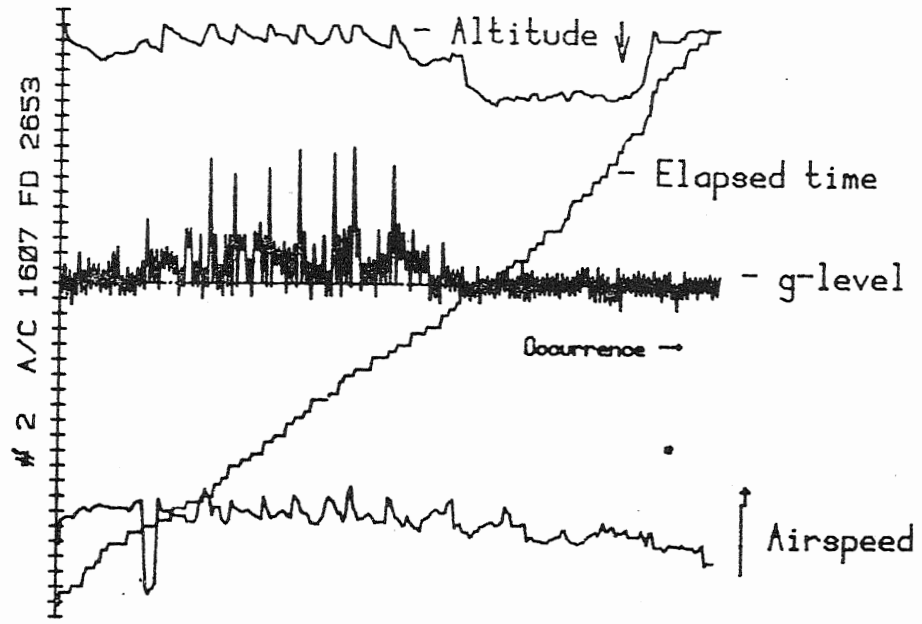

Fig. 9 - Sequence of g-levels with associated altitude, airspeed and elapsed time. Data for a typical flight

Fig.10. Software was developed for fully automated FCG testing with provision for control of stress level as well as a pre-assigned function of stress intensity factor with crack length. Computer estimates crack length by measuring unloading compliance using a crack opening displacement gage and referring to a calibration table of compliance versus crack length. The crack opening displacement gage developed for crack growth testing is shown in Fig.11. In K-Controlled testing the computer after each measurement of crack length adjusts the load level to obtain the required stress intensity factor. Fig.12 shows the flow chart for K-Controlled testing. Extensive S mean and K mean controlled fatigue crack growth tests have been carried out under flight-by-flight spectrum loading of fighter aircraft. All tests have been carried out on single edge notched specimen of Al-Cu-Mg and Al-Zn-Mg alloys. Some of the interesting results obtained will be discussed in a later section. Fig.13 shows a typical flight loading imposed on specimen under spectrum loading.

The testing software developed has been recently expanded and optimised to include automated crack opening stress measurement and to reduce test time by eliminating stress peak levels which are below crack opening stress level and stress ranges which produce stress intensity range below threshold. The fully automated estimation of crack closure and opening stress levels during a fatigue crack growth test uses an iterative least square analysis algorithm developed earlier to analyse crack growth rate data. The method is schematically described in Fig.14. It requires application of a complete load cycle each time a measurement is to be carried out. This crack closing/opening load determination cycle is a slow downward ramp (0.5 Hz) starting from a load level at which the crack is certain to be open (Maximum stress in case of a constant amplitude sequence). During this ramp, load and COD sampled every 10 MS are stored (a total of about 200 points). The downward excursion stops at zero load. A machine code routine then uses the algorithm in Fig.14 to process data to determine the load level corresponding to crack closure. This is followed by an upward ramp during and after which the same exercise is repeated to determine crack opening load level. The entire cycle takes about 2 seconds of real time (the time taken for the iterative least square analysis is a fraction of a second). The procedure includes logic to exclude obviously incorrect estimates. For example, the estimate is considered invalid if compliance does not increase with crack length.

At the conclusion of the test, crack opening and closing load levels are recorded alongside crack length and number of blocks in the table of test results. These form part of the FCP Data Bank file on disk storage. This feature permits a more meaningful analysis of test results. Under constant amplitude loading, crack closure data permit correlation of stress ratio effects. Under spectrum loading, they provide a basis for explaining load interaction effects. Implementation of the proposed Sop determination technique appears to be an attractive prospect. It must be pointed however that it has certain intrinsic limitations associated with the mounting of the gage. As the crack grows away from the edge (a 15 mm), the Sop estimates tend to become more and more unreliable as will be seen in data presented below. Further, the accuracy of the technique even at small crack lengths requires validation using other proven techniques. It is proposed to carry out such an exercise using the electron fractography technique proposed by Sunder and Dash (1982).

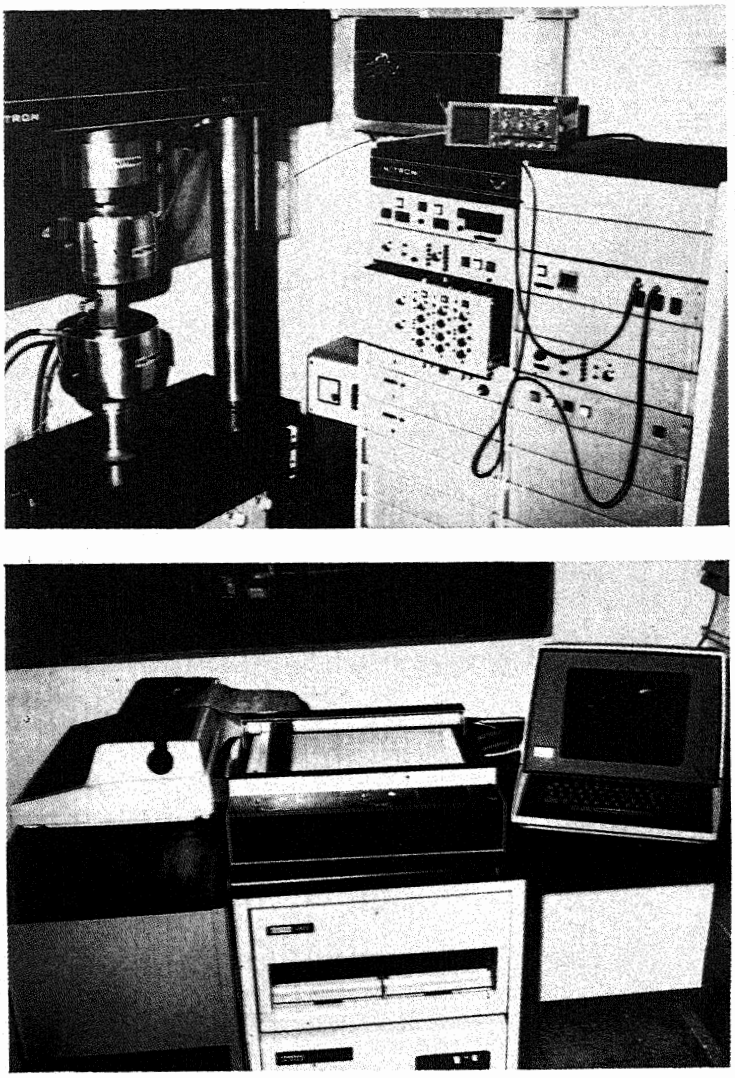

FIG 10 INSTRON - 1343 COMPUTER (PDP 11-23) CONTROLLED TESTING MACHINE

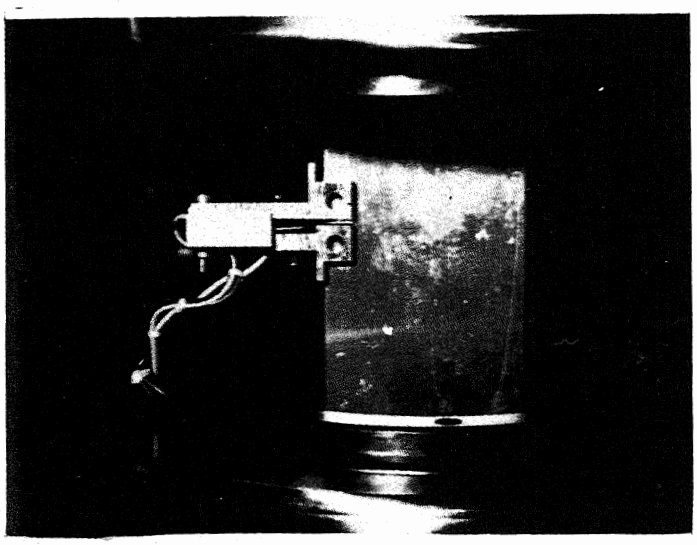

FIG 11 C.O.D. GAGE MOUNTED ON EDGE CRACKED SPECIMEN TO MONITOR CRACK LENGTH IN AUTOMATED FATIGUE CRACK GROWTH TESTING

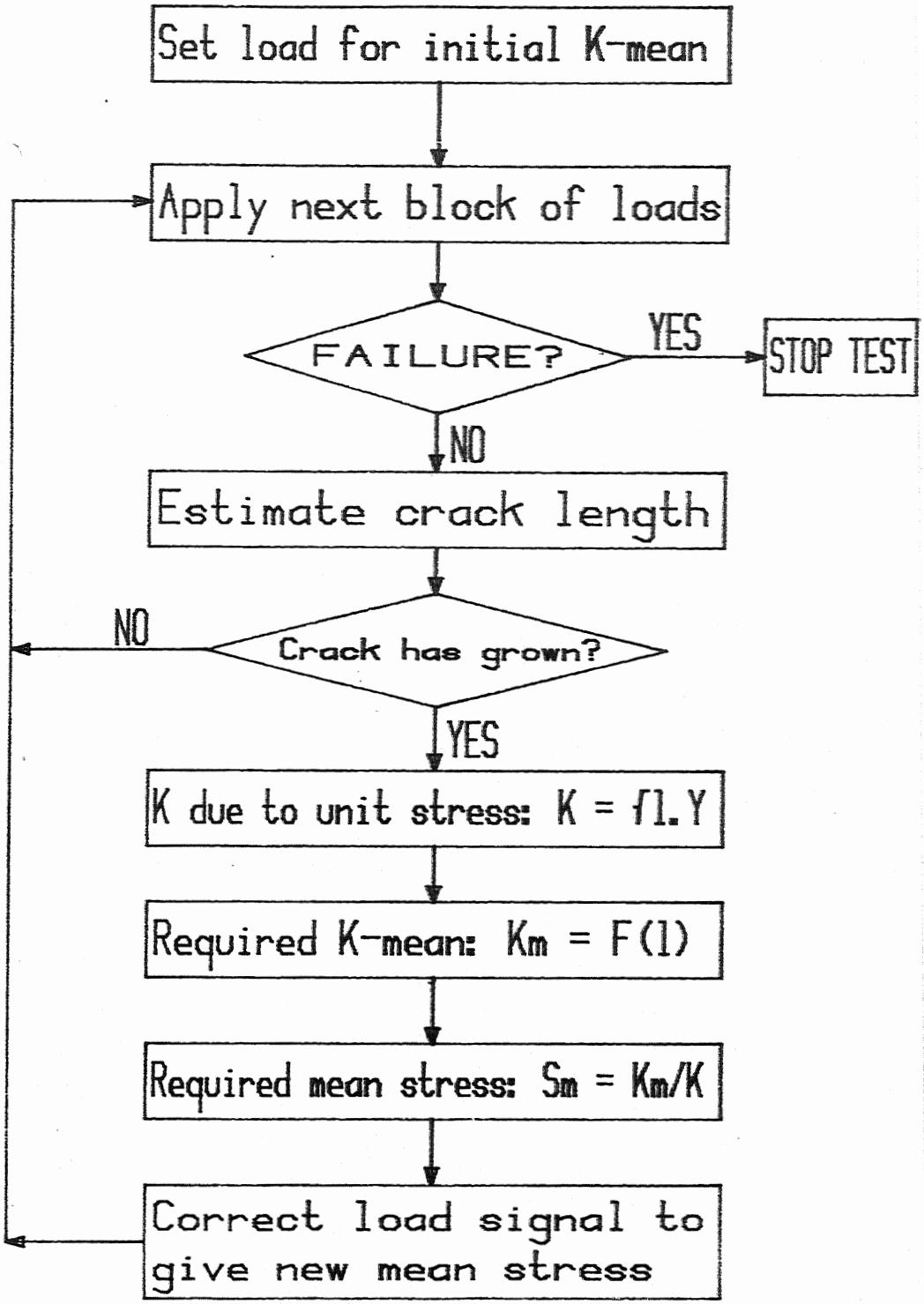

FIG 12 FLOW CHART FOR K-CONTROLLED AUTOMATED FATIGUE CRACK GROWTH TESTING

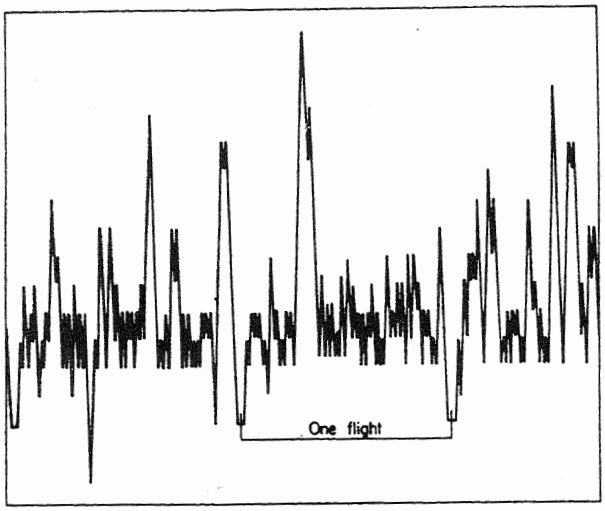

FIG 13 TYPICAL SEQUENCE OF LOADS ON A COMBAT AIRCRAFT

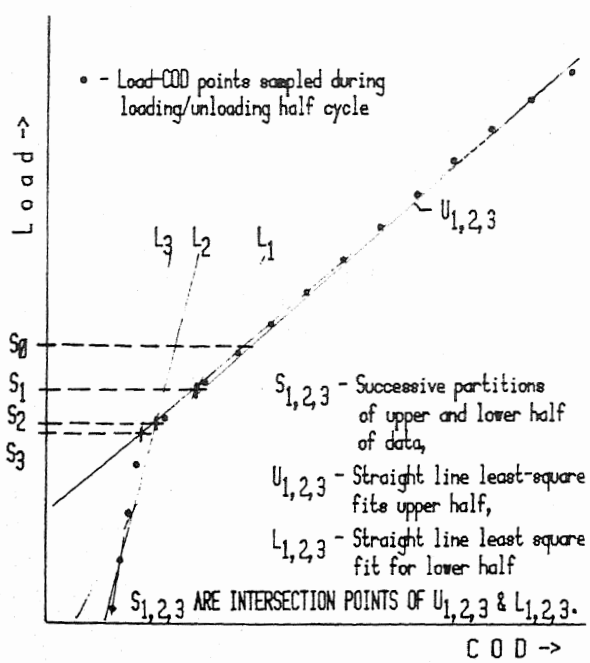

FIG 14 ITERATIVE TECHNIQUE FOR AUTOMATED CRACK CLOSURE STRESS MEASUREMENT

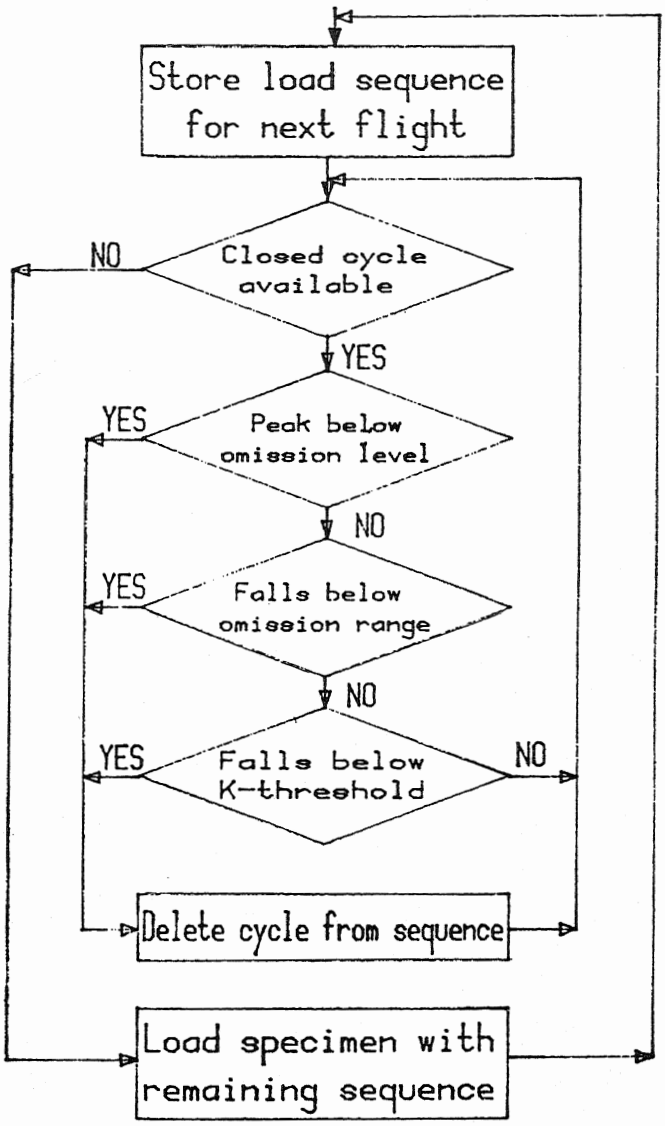

FIG 15 FLOW-CHART FOR ON-LINE FATIGUE ANALYSIS

The elimination of stress levels which are below the crack opening stress level and of stress ranges which give raise to ΔK levels below threshold, during a test requires on line fatigue cycle analysis. The omission levels needs constant readjustment since the crack length is changing. The process is to eliminate the below threshold excursions in the Markov matrix of occurrences of range and peak level combinations derived from the Markov matrix of excursions by rainflow cycle counting method. Fig.15 shows the flow chart for on line fatigue analysis used for eliminating load peaks which fall below the omission level (i.e., crack opening level) and load cycle ranges which fall below the omission range (determined from threshold ΔK considerations). Full details of this technique has been reported by Sunder, 1984.

(II) ANALYTICAL AND EXPERIMENTAL STUDIES IN FRACTURE MECHANICS AND FATIGUE CRACK GROWTH

(A) ANALYTICAL STUDIES

Analytical studies carried out in fracture mechanics and fatigue crack growth are generally in the following areas.

(1) Determination of stress intensity factors

(2) Development of computer software for generating S-N curves for spectrum loading

(3) Studies on variability in fatigue life due to strengthening mods applied to aircraft in service

(4) Studies on plastic energy dissipation rate during stable crack growth under biaxial loading

(5) Modelling of stable crack growth under monotonically increasing applied stress using energy balance considerations

(6) Development of unified approach to modelling fatigue crack growth based on energy balance considerations.

(A.1) Determination of stress intensity factor

(i) Cracked isotropic and laminated anisotropic cylindrical shells: (Laxminarayana & co-workers 1982, Murthy and co-workers 1981)

While the problem of cracks in shells has been treated in the past exclusively by integral equation methods, an alternative technique based on differential equation approach has been successfully used to obtain stress intensity factors for through the thickness cracks in isotropic cylindrical shells. Perturbation solutions in the curvature parameter have been obtained for symmetric as well as arbitrarily oriented cracks. These are quite accurate for small values of curvature parameter. Numerical solutions have been obtained for large values of curvature parameter by satisfying the crack surface boundary conditions using numerical procedures. An elegant transformation technique has been used to transform the solution in elliptic co-ordinates to local polar co-ordinates centred at the crack tip in order to recover the singular stress field in a form

convenient for evaluating stress intensity factors.

Charts have been developed from which mode I and mode II components of both membrane and bending stress intensity factors can be directly obtained over a wide practical range of the parameter involved. Fig.16 shows some typical results.

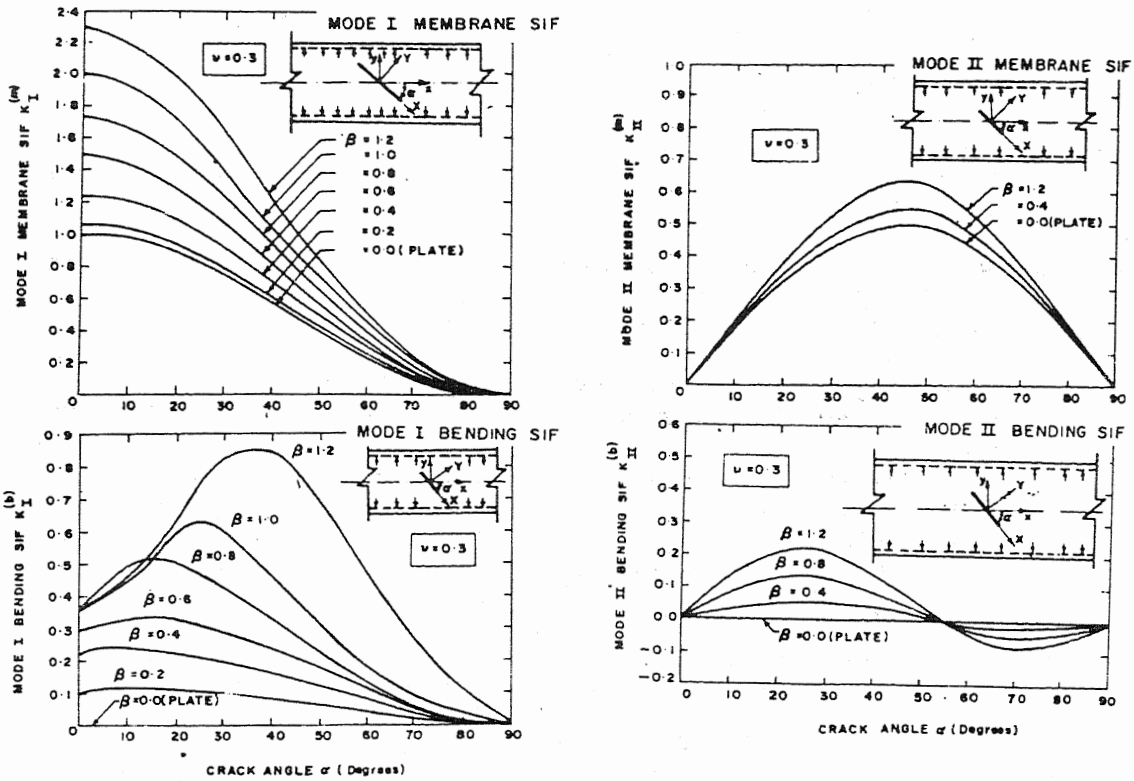

FIG 16 STRESS INTENSITY FACTORS FOR ARBITRARILY ORIENTED CRACKS IN PRESSURISED CYLINDRICAL SHELLS

A finite element model for the analysis of laminated composite cylindrical shell and flat plates with through the thickness cracks has been developed. Analysis takes into account anisotropic elastic behaviour, bending extensional coupling and transverse shear deformation effects. The parabolic isoparametric cylindrical shell elements (both singular and regular elements) used in this model employ independent displacement and rotation interpolation in the shell middle surface.

(ii) Cracked plates in bending
(Hartranft and Sih 1968, Viswanath and co-workers 1984)

A general solution has been developed for the symmetric bending

stress distribution at the tip of a crack in a homogeneous isotropic plate taking shear deformation into account through Reissner's theory. The solution obtained is in terms of polar co-ordinates at the crack tip and include the complete class of solutions satisfying all the three boundary conditions along the crack. Typical results are shown in Fig.17 for a square plate with a centre crack subjected to bending. Using these solutions in a finite element technique, a method has been developed to solve any problem of bending of cracked plates without any restrictions on the value of the thickness to crack length ratio.

Recently the effect of crack face bearing on stress intensity factors for a cracked plate under bending loads has been taken into account.

(A.2) Development of computer software for generating S-N curves for spectrum loading

Landgraf and co-workers 1977, Sunder 1982, Sunder and Raju 1984)

Engineering structures and machine components often experience complex sequence of service loads. Local cyclic stresses and strains at the root of notches (stress concentrations) determine the progressive accumulation of fatigue damage. As shown in Fig.18 notch root mean stress and mean strain can be load sequence sensitive. This aspect of notch root material behaviour can be accounted for if the local stress-strain approach is used for fatigue analysis. This procedure is schamatically described in Fig.19. It is normally implemented on high speed digital computers which permit rapid cycle-by-cycle fatigue analysis over thousands of fatigue load cycles. This is a widely used technique in the automobile and aircraft industries.

Computer based fatigue analysis can also be used to generate S-N curves for spectrum loading. Such curves provide a direct reference for the fatigue designer in design stress notch factor trade offs. The format of such curves is shown in Fig.20. Computer software has been developed for computer generation of spectrum loading S-N curves. The software includes elements which contribute to high computation speed with moderate memory requirements. This activity is described in detail by Sunder, 1982.

(A.3) Studies on variability in fatigue life due to strengthening mods applied to aircraft in service

(Dash 1983)

Strengthening mods at fatigue critical areas indicated in a full scale fatigue test have to be necessarily applied to aircraft in service to achieve the required fatigue lives at these areas. Essentially, strengthening mods bring down the stress levels at the areas where they are applied and thus improve the fatigue life. The achieved safe life depends on the stage in service life at which the strengthening mod is applied and also the variability in the effectiveness of the strengthening mod in reducing the stresses. The effectiveness of the strengthening mod or patch is defined by the so called patch factor given by

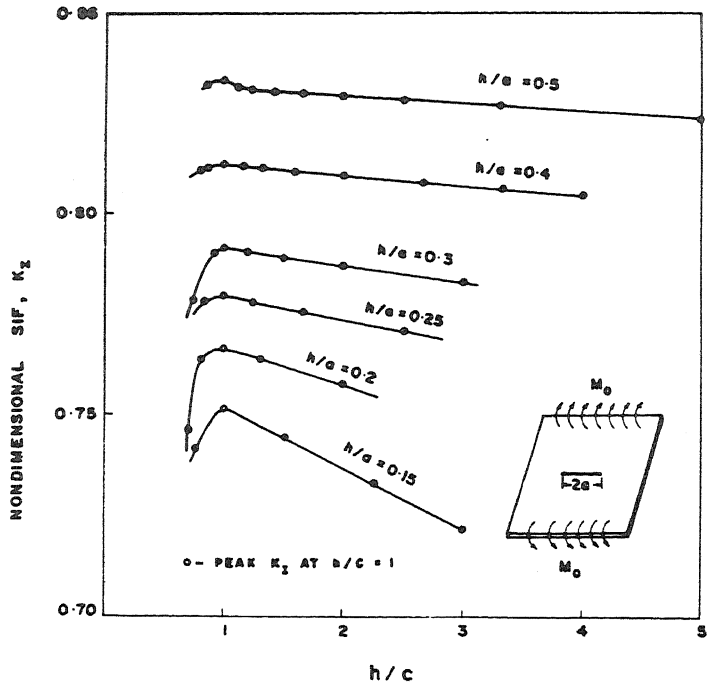

VARIATION OF STRESS INTENSITY FACTOR WITH h/C RATIO

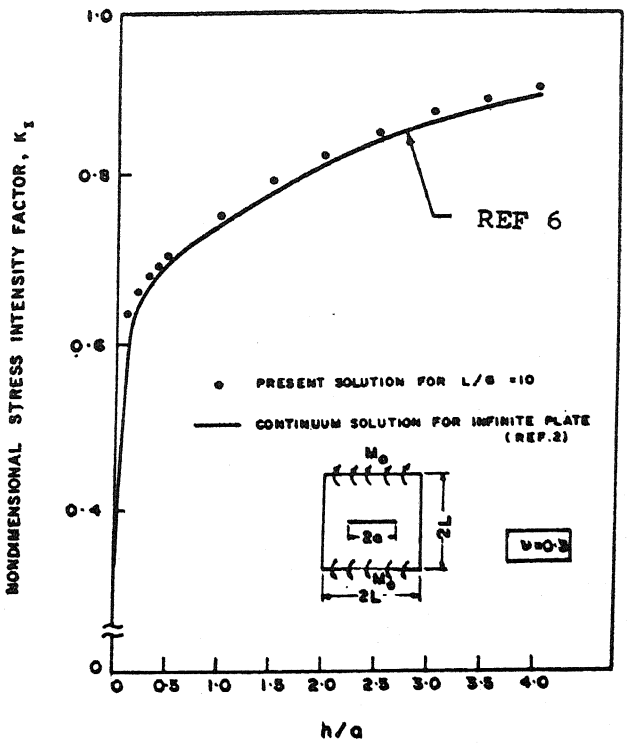

STRESS INTENSITY FACTOR Vs h/a RATIO

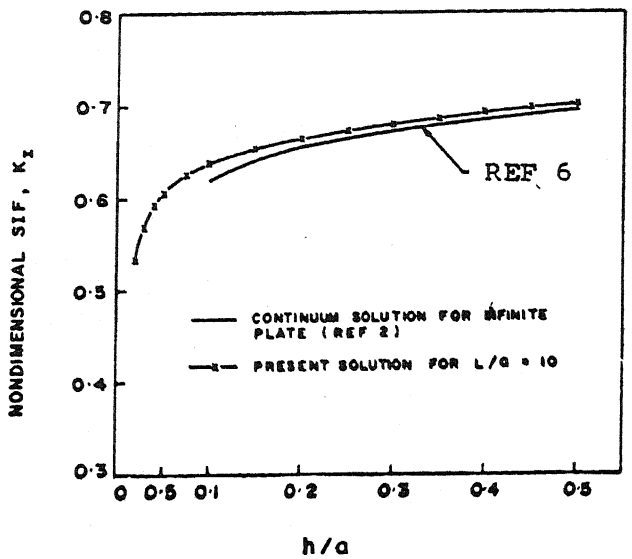

STRESS INTENSITY FACTOR Vs h/a RATIO

FIG 17 STRESS INTENSITY FACTORS FOR FINITE SIZE CENTRE CRACKED PLATES UNDER BENDING OBTAINED BY FINITE ELEMENT ANALYSIS BASED ON HIGHER ORDER PLATE THEORY.

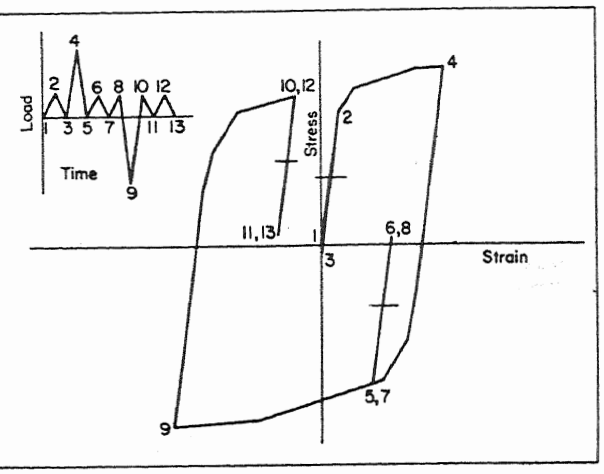

FIG 18 NOTCH ROOT MEAN STRESS-STRAIN CAN BE SENSITIVE TO LOAD SEQUENCE.

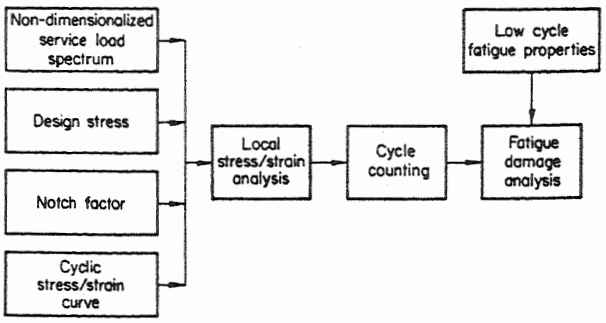

FIG 19

FATIGUE ANALYSIS USING LOCAL STRESS-STRAIN APPROACH

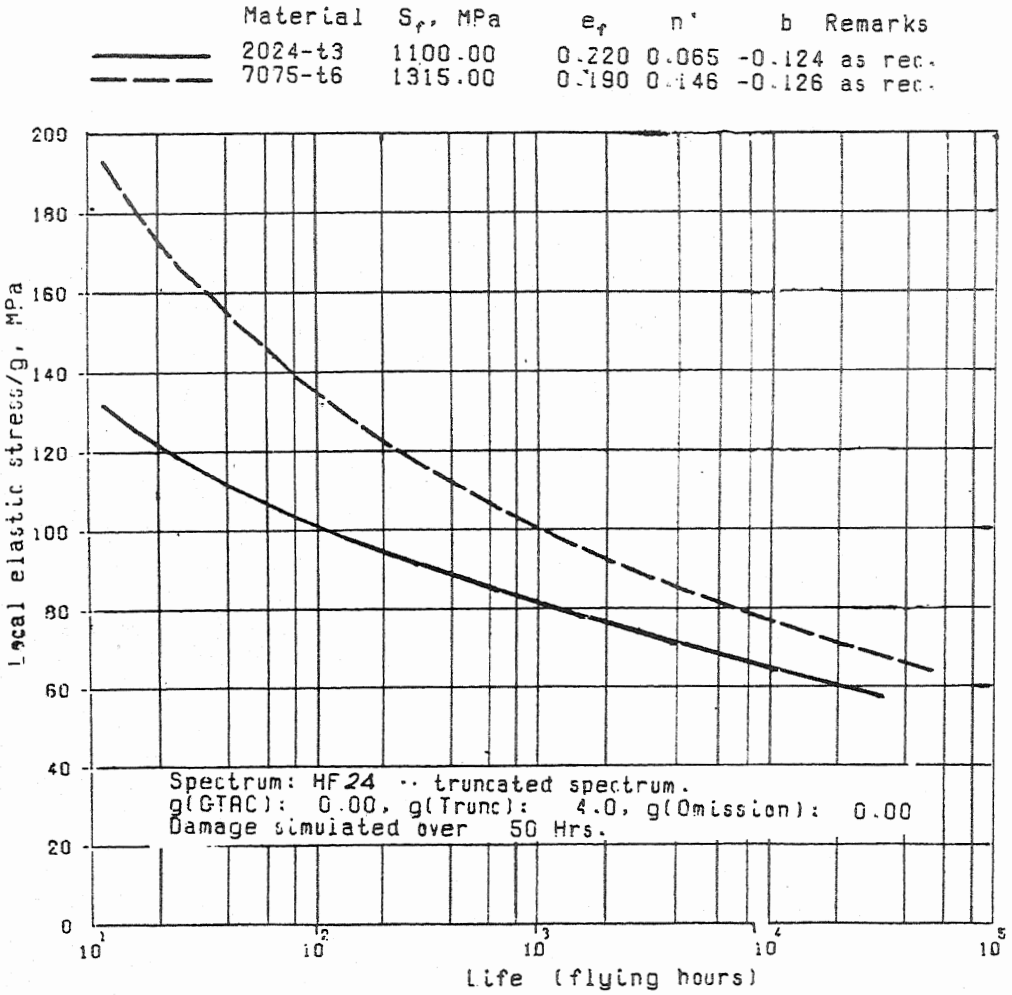

FIG 20 TYPICAL SPECTRUM S-N CURVES GENERATED BY FATIGUE ANALYSIS BASED ON LOCAL STRESS-STRAIN APPROACH

$$\text{Patch factor} \quad Pf = \frac{\text{Stress with the patch}}{\text{Stress without the patch}}$$

The safe life with a strengthening patch has been obtained as a function of the service life at which the patch is applied expressed as a fraction of the safe life with the patch. The influence of patch factor variability load spectrum variability etc. on the safe life has been investigated. Fig.21 shows some typical results.

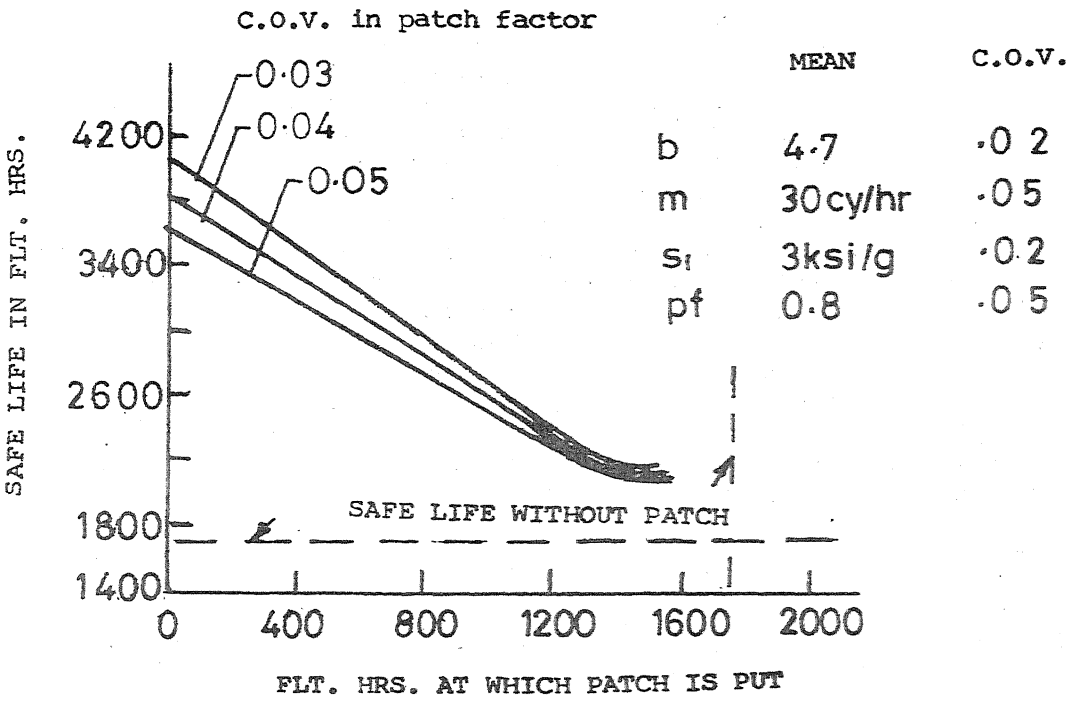

FIG 21 EFFECT OF VARIABILITY IN PATCH FACTOR ON SAFE-LIFE

(A.4) Analysis of plastic energy dissipation rate during stable crack growth

(Raju 1979, 1980, Raju and Dash 1979)

It has been recognised that the plastic deformation field at the tip of a crack extending under increasing applied stress is different from the plastic deformation field at the tip of a stationary crack subjected to an increasing applied stress. This difference arises due to the fact that crack extension brings about unloading in certain regions close to the crack tip while the stress and strains increase in other regiona. The extent of unloading depends on the rate of change of applied stress

with respect to crack length or crack extension. This was first recognised by Valluri (1965) in his early work. Considering these aspects an analysis has been made for plastic energy dissipation rate during stable crack growth under K-controlled small scale yielding conditions using a quasi-stationary approache for equi-biaxial loading (Raju 1969, 1980) Plastic energy dissipation rate obtained in a non-dimensionalised form has been found to be a function of the stable crack growth parameter which is nothing but the rate of change of plastic zone size with crack length, and stress-strain curve parameters such as the strain hardening coefficient. It is to be noted that the rate of change of plastic zone size with crack length is also a function of the rate of change of applied stress with crack extension. In obtaining plastic energy dissipation rate, the energy dissipated in a small fracture process zone in the immediate vicinity of the crack tip and located within the plastic zone is not considered as deformation in the zone is highly inhomogeneous due to the fracture processes active in the zone. The boundary of the fracture process zone (FPZ) is assumed to be defined by a critical value of stress or strain. Effect of biaxial loading conditions on plastic energy dissipation rate during stable crack growth has also been studied for K-controlled small scale yielding conditions. In this case the non-dimensionalised plastic energy dissipation rate is a function of rate of change of plastic zone length with crack extension, C_0, biaxial stress ratio, λ , (i.e., ratio of stress applied parallel to the crack to the stress applied normal to the crack plane), the ratio of the applied stress normal to the crack plane to the yield strength, $\overline{\sigma}$, and the material stress strain parameters such as strain hardening coefficient. An interesting aspect is that the plastic energy dissipation rate depends on the applied stress path defined by the variation of the applied stress in the direction normal to crack plane, with respect to the applied stress in the direction parallel to the crack. Fig.22 shows typical results obtained for non-equibiaxial loading conditions (Raju and Dash 1979, Raju 1980).

(A.5) Modelling of stable crack growth under monotonically increasing applied stress using energy balance considerations
(Raju 1980, 1979)

In the case of a stationary crack with progressively increasing plastic zone under a monotonic increase in applied stress, the rate of energy absorbed in the plastic zone is equal to the rate of energy release due to the plastic zone. This idea has been used to set up an energy balance equation governing energy changes due to growing plastic zone at a stationary crack tip under monotonic increase in applied stress. A critical level of energy absorbed in a fracture process zone (FPZ) inside the plastic zone is taken as the condition for the onset of crack extension. The subsequent stable crack growth phase is assumed to be controlled by constant rate of flow of energy into the fracture process zone. The rate of flow of energy into the fracture process zone is equal to the energy release rate minus the rate of energy absorbed in the plastic zone outside of the FPZ. Thus the plastic zone acts

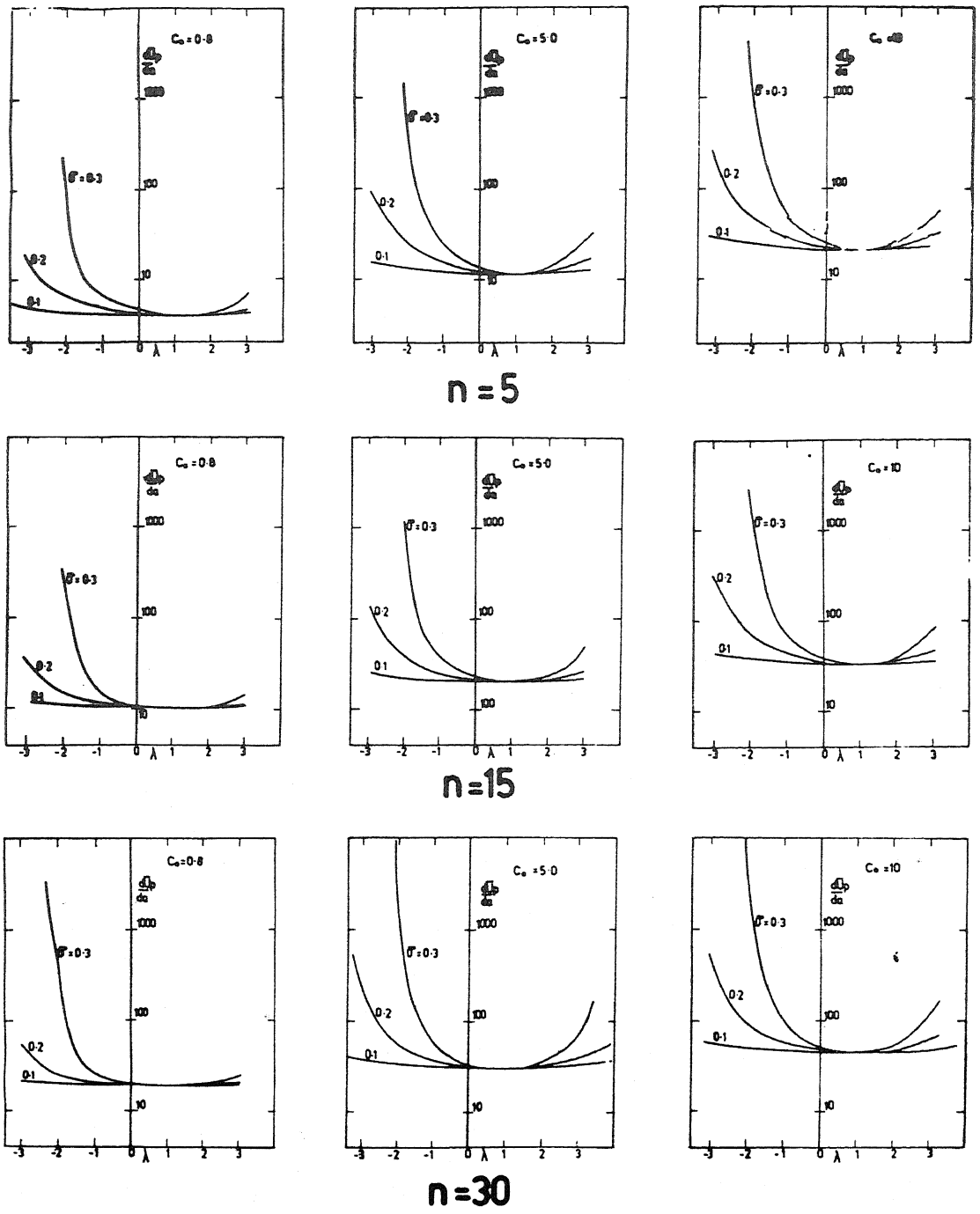

n: Inverse of strain hardening coefficient ; $C_o = \frac{\partial \omega_{po}}{\partial \bar{\sigma}} \cdot \frac{d\bar{\sigma}}{da} + \frac{\partial \omega_{po}}{\partial a}$; $\lambda : \sigma_y / \sigma_x$

$\bar{\sigma} : \sigma_y / \sigma_{yp}$.

FIG. 22 VARIATION OF NORMALISED PLASTIC ENERGY DISSIPATION RATE $d\bar{U}_p/da$ WITH BIAXIAL STRESS RATIO λ FOR DIFFERENT VALUES OF $\bar{\sigma}$, C_o AND n AT ξ_{fo} = 1.6 AND Ω_{eff} = 0

as an energy shield for flow of energy into the FPZ. Such an idea was first proposed by Havner (1966) and subsequently by Broberg (1975). Using these concepts an energy balance equation governing thestable crack growth phase has been set up and solved to obtain stable crack growth curves for an infinite plate with a central crack subjected to increasing stess normal to the crack plane applied at infinity. Fig.23 shows some typical stable growth curves obtained indicating the effects of initial crack length, and plastic zone size at onset of crack extension.

(A.6) Development of unified approach to modelling fatigue crack growth based on energy balance considerations

Models of fatigue crack growth under constant amplitude loading can be broadly classified into four groups.

Group 1: Models based on crack tip stress, strain or displacement governing crack extension. In this group of models, crack growth is related to:

1. Strain hardening to fracture of a volume of material at the crack tip proportional to plastic zone size (Head, 1953; McEvily and Illg, 1959; Valluri, 1961; Valluri and others, 1963).
2. A critical stress or strain being attained at a point ahead of the crack tip and distance of this point from the crack tip (Weiss, 1964; Krafft, 1964, 1965).
3. Accumulation of plastic strain or displacement to a critical value and the distance at which this value is reached (Weertman, 1969, 1973).
4. Plastic opening displacement at the crack tip or geometry change based on the process of crack tip blunting and resharpening or the process of alternating slip on ±45° planes or decohesion along ±45° shear bands at the crack tip (Laird and Smith, 1962; Frost and Dixon, 1967; Neumann 1967, 1974; Lardner, 1968; Tomkins, 1968, 1969; Pelloux, 1970; Donahue and co-workers, 1972; Schwalbe, 1973, 1974; McEvily, 1974; Kuo and Liu, 1976; McEvily and co-workers, 1976; Kanninen and co-workers, 1977).
5. Local strain energy density or energy release rate (Paris and co-workers, 1961; Barsom, 1971; Sih and Barthelemy, 1980; Badaliance, 1980).

Group 2: Models based on cumulative damage governing crack extension. In these models damage is estimated using low cycle fatigue relationships. It is postulated that crack extends as a consequence of the accumulation of damage in the material ahead of the crack tip experiencing cyclic plastic strains (McClintock, 1963; Yokobori and Ichikawa, 1968; Liu and Iino, 1969; Yokobori and co-workers, 1969; Fleck and Anderson, 1969; Majumdar and Morrow, 1974; Antolovich and co-workers, 1975; Duggan, 1977; Cioclov, 1977; Lal and Garg, 1977; Homma and Nakazawa, 1978; Duggan and Chandler, 1979; Proctor and Duggan, 1979; Stouffer and Williams, 1979).

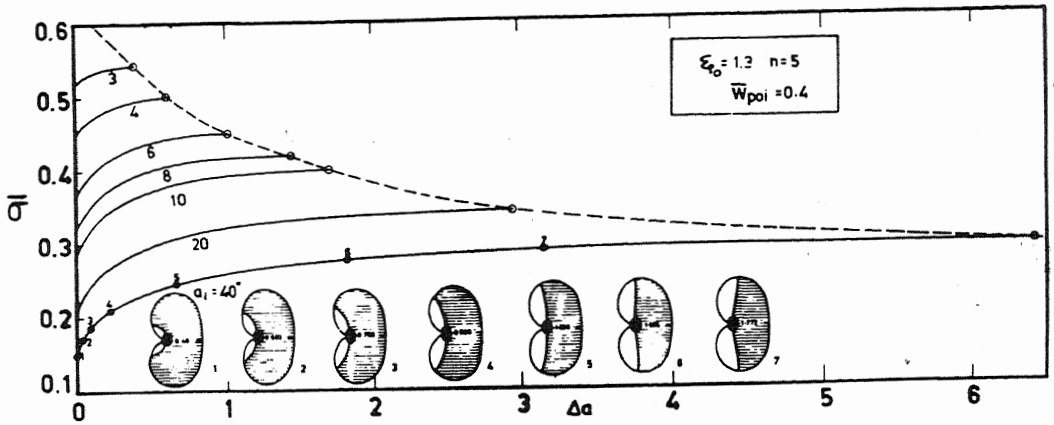

EFFECT OF INITIAL CRACK LENGTH

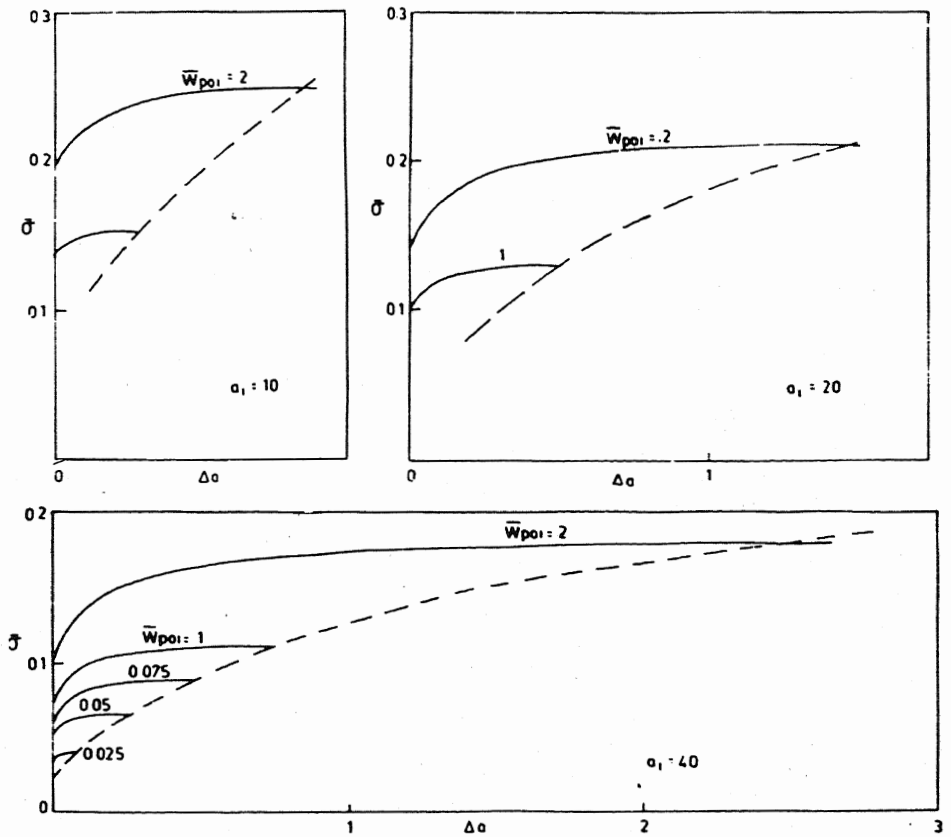

EFFECT OF PLASTIC ZONE SIZE AT ONSET OF STABLE CRACK GROWTH

FIG 16 STABLE CRACK GROWTH CURVES SHOWING EFFECT OF INITIAL CRACK LENGTH AND PLASTIC ZONE SIZE AT ONSET OF STABLE CRACK GROWTH

Group 3: Models based on critical level of energy absorption or energy balance. In these models, crack growth rate is related either to hysteresis energy absorbed in the cyclic plastic enclave or to considerations of energy balance (Liu 1963; Rice, 1967; Gallina and co-workers, 1967; Paris, 1969; Wnuk, 1971, 1973; Raju, 1972; Cherepanov and Halmonov, 1972; Mura and Lin, 1974; Ikeda and co-workers, 1977; Weertman, 1978; Izumi and Fine, 1979; Raju, 1980, 1983).

Group 4: Models based on R-curve concepts evolved to explain stable crack growth under monotonic loading. In these models crack extension in each cycle is equal to stable crack growth increment under the rising half cycle as estimated using K_R or J_R curve approach (Musuva and Radon, 1979, 1980; Rhodes and co-workers 1981).

In addition to crack growth rate equations from these models, a number of empirical relationships as a function of K or J-integral have been proposed (Forman and coworkers, 1967; Pearson, 1972; Heald and others, 1972; Richards and Lindley, 1972; Saxena and others, 1978; Collipriest, 1972).

It is appropriate here to recognise that the discovery of crack closure phenomenon (Elber, 1970) represents an important milestone in the understanding of the mechanics of crack growth. It has resulted in modifications to existing equations, often in an empirical manner. The effect of stress ratio at intermediate range crack growth rates was explained on the basis of crack closure by Elber. Crack closure also explains retardation and acceleration effects observed under variable amplitude loading. More recently, it has been shown that crack closure can explain decrease in near threshold crack growth rates due to aggressive environment and the effect of stress ratio on threshold stress intensity (Ritchie and others, 1980; Paris and others, 1972).

It is not intended here to comprehensively review the various models of fatigue crack growth. Many reviews of the various models of crack growth are available in the literature (Rice, 1967; Grosskreutz, 1971; Schwalbe, 1974; Maddox, 1975). Efforts have been made to model short crack growth behaviour by observing the relation between the threshold stress intensity range and the fatigue endurance limit (Topper and Haddad, 1982).

An overview of various models indicates that a large number of them, notably of Group 1 do not account for stress ratio, fracture toughness, thickness, etc. The basis of most models does not permit in their present form considerations of the effects of various parameters on fatigue crack growth rates in an unified manner. An unified model capable of accounting for a number of parameters on crack growth under constant amplitude loading has been developed (Raju, 1980, 1983).

Unified model of fatigue crack growth

A detailed description of the basis of this model is available elsewhere (Raju, 1972, 1980, 1983). Let us consider the plastic deformation history

at the tip of a crack growing under tensile constant amplitude loading with and without crack closure effects. For a crack growing in each cycle under fatigue, plastic deformation history consists of hysteretic (cyclic) and non-hysteretic (monotonic) components. Hysteretic or cyclic plastic deformation occurs in an inner plastic zone referred to as cyclic plastic zone. Non-hysteretic or monotonic plastic deformation occurs in an outer, monotonic plastic zone. Monotonic plastic deformation occurs as a consequence of crack extension. Obviously, for a stationary crack, there will be no monotonic plastic deformation after the first rising half cycle. Crack extension at any stage of loading increases the stresses, causing additional plastic deformation in some areas near the crack tip and decreases stresses causing elastic unloading in other areas. Consequently, the effect of crack extension in each cycle is to increase the hysteresis loop in some areas and decrease it in the remaining areas within the cyclic plastic zone. For the same reason, the monotonic plastic zone will be different for a growing crack as opposed to a stationary crack under monotonic loading. It has been observed that there is no difference in the hysteresis energy absorbed in the cyclic plastic zone between a growing and a stationary crack. It was also noted that material elements at the tip of a growing crack would have experienced a prior history of monotonic and cyclic plastic deformation which would have caused damage resulting in a reduction of fracture energy. It is reasonable to assume that the reduction in fracture energy is proportional to the hysteresis energy absorbed per cycle.

The effect of crack closure is to reduce the cyclic plastic zone size and associated range of cyclic plastic strain experienced by the material in the crack tip region. Fig.24 shows the deformation history in various regions of the cyclic and monotonic plastic zones with effect of crack closure. The neutral lines separating the regions of elastic unloading from the rest of the plastic zone are also shown in the figure. Parts of the crack lips immediately behind the crack tip deform in compression during the unloading half-cycle.

The important effect of crack closure is the drastic reduction in the size of the cyclic plastic zone which is a function of the effective stress intensity range, ΔK_e. Crack closure reduces the hysteresis energy absorbed in each cycle.

Energy balance in fatigue crack growth

The changes in external work, elastic strain energy and energy of plastic deformation in the plastic zone are considered in constructing an equation of energy balance. As mentioned earlier, the crack tip having been in a damaged state due to prior plastic deformation history will require less energy for fracture or for crack extension. The nature of damage may be in the form of voids or microcracks nucleated at boundaries of second phase particles which will attract easy slip and the crack may extend by slip plane decohesion. The crack may also extend by cleavage or ductile fracture of crack tip material depending on the environment and the stress intensity range.

The energy balance equation can be written as

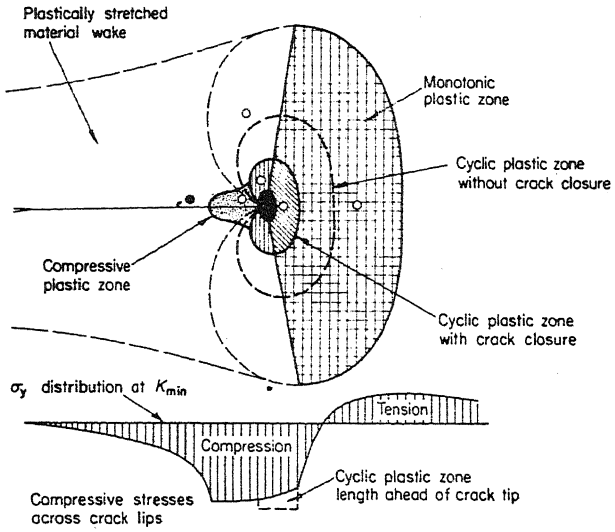

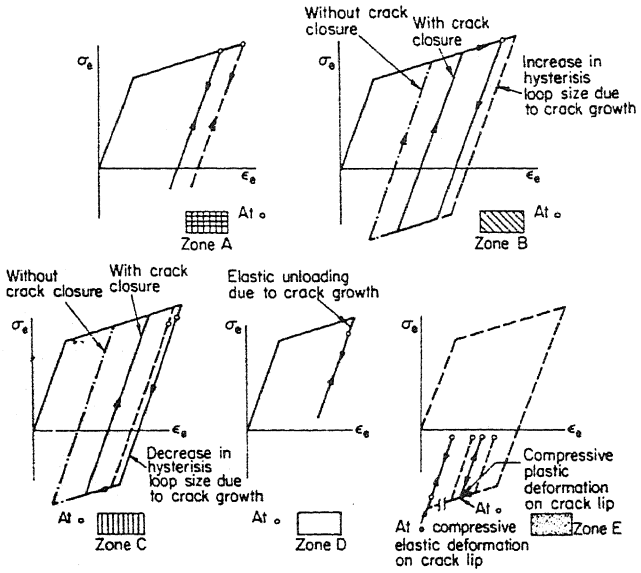

IG 24 CYCLIC STRESS-STRAIN HISTORY AT THE TIP OF A GROWING UNDER CONSTANT AMPLITUDE LOADING, (CRACK CLOSURE CONSIDERED)

$$(dW_{ext}/da)(da/dN) - (dU_e/da)\cdot(da/dN) - (dU_P/da)\cdot(da/dN) = U_f'(da/dN) - \beta \tilde{U}_P \quad -- 1$$

where da/dN is the crack growth rate (dWext/da)(da/dN) is the change in external work in each cycle due to crack extension, (dUe/da)(da/dN) is the change in strain energy in each cycle due to crack extension, (dUp/da)(da/dN) is the change in the energy of plastic deformation in each cycle due to crack extension.

The left and side of the equation of energy balance represents the net energy available in each cycle for fracture or crack extension process. The right hand side represents energy required for fracture or crack extension after taking into account prior hysteretic plastic deformation. The term $\beta \tilde{U}_p$ is the reduction in energy required for crack extension, U_f da/dN per cycle due to prior deformation history. Hysteresis energy may to a considerable extent be dissipated as heat.

β reflects the fraction of this energy contributing to damage. The reduction in energy required for crack extension may also depend on monotonic (nonhysteretic) plastic deformation. Nonhysteretic plastic energy may contribute directly to damage or increase damage due to hysteretic energy. The terms on the left indicate nonhysteretic deformation energy is the same as in the case of crack extension under monotonic loading. Influence of nonhysteretic plastic energy on damage due to hysteretic energy is accounted for by taking β as

$$\beta = A \left(\frac{W_P}{\tilde{W}_P} \right)^n \quad -- 2$$

Using the relation between Wp and $\tilde{W}_p$, the expression simplifies to

$$\beta = 2A\gamma^{2n}(1-Re)^{-2n}$$

where γ is the ratio of the yield stress range to the monotonic yield stress, Re is the effective stress ratio, (Sop/Smax). Substituting $2A\gamma^{2n} = \bar{A}$, 2n = m, one gets

$$\beta = \bar{A}(1-Re)^{-m} \quad -- 3$$

The hysteretic plastic energy absorbed in the cyclic plastic zone in each cycle is shown to be

$$\tilde{U}_P = (B/E)\,\tilde{S}_{yp}^2\,\tilde{W}_P^2 \quad -- 4$$

where B is a constant depending on the strain hardening coefficient. From (1), we obtain the following expression for crack growth rate

$$\frac{da}{dN} = \frac{\bar{A}\,(1-Re)^{-m}\,(B/E)\,\tilde{S}_{yp}^{2}\,\tilde{W}_{p}^{2}}{U_f' - (dW_{ext}/da - dU_e/da - dU_p/da)} \qquad --5$$

U_f - (dWext/da - dUe/da - dUp/da) = 0 represents the energy balance equation governing fracture under monotonic loading or fracture instability. For LEFM conditions, the crack growth relation can be written as

$$\frac{da}{dN} = \frac{\bar{A}_1\,(1-Re)^{-m}\,\Delta K_e^{4}}{K_c^2 - K_{max}^2} \qquad --6$$

In the above relation it is assumed that hysteretic plastic energy absorbed in the entire cyclic plastic zone contributes to reduction in fracture energy. If one considers that the hysteretic plastic energy absorbed in a narrow strip in line with the crack and in the cyclic plastic zone is effective in reducing the fracture energy, while the hysteresis energy absorbed elsewhere in the cyclic plastic zone is dissipated as heat, the growth rate relation is obtained for LEFM condition as

$$\frac{da}{dN} = \frac{\bar{A}_{1s}\,(1-Re)^{-m}\,\Delta K_e^{2}}{K_c^2 - K_{max}^2} \qquad --7$$

The growth rate relations (6) and (7) assume that the hysteresis energy absorbed in the entire cyclic plastic zone contributes to fracture energy reduction and that the hysteresis energy absorbed in a narrow strip in the cyclic plastic zone is effective in reducing fracture energy. These two assumptions represent extreme conditions. The actual situation will be in between. It follows that

$$\frac{da}{dN} = \frac{A_{1g}\,(1-Re)^{-m}\,\Delta K_e^{p}}{K_c^2 - K_{max}^2} \qquad --8$$

where the exponent p will be between 2 and 4 and Kc is plane stress fracture toughness.

So far, in deriving the growth rate relations, plane stress conditions were assumed. Reduction in fracture due to absorbed hysteresis energy would be greater for plane strain conditions. Taking this into account, we get the following relationship for plane strain conditions

$$\frac{da}{dN} = \frac{A_{2g}\,(1-\bar{R}e)^{-m}\,\Delta \bar{K}_e^{p}\,(1-2\nu)^{p}}{K_{Ic}^2 - K_{max}^2} \qquad --9$$

It is to be noted that A_{2g} is greater than A_{1g} reflecting the effects of triaxial tension and higher tensile stresses normal to the crack plane.

The growth rate relations can be modified to include threshold effects as

$$\frac{da}{dN} = \frac{A_{1g}(1-R_e)^{-m}(\Delta K_e - \Delta K_{th})^{p}}{K_c^2 - K_{max}^2} \quad -- 10$$

$$\frac{da}{dN} = \frac{A_{2g}(1-\bar{R}_e)^{-m}(1-2\nu)^{p}(\Delta \bar{K}_e - \Delta \bar{K}_{th})^{p}}{K_{IC}^2 - K_{max}^2} \quad -- 11$$

where, $\bar{R}e$ is the effective stress ratio, $\Delta \bar{K}e$ is effective stress intensity range, $\Delta \bar{K}_{th}$ - the threshold stress intensity range for plane strain conditions, K_{IC} - is the plane strain fracture toughness.

It is interesting to note here that the effect of stress ratio at lower growth rates is governed by crack closure, while at high growth rates, it is controlled by fracture instability conditions. There could be situations where at low growth rates, stress ratio effects are evident even though crack closure is absent. The term $(1-Re)^{-m}$ accounts for this possibility. Fig.25 shows the effect of stress ratio as predicted by the above relation (plane stress case) with m=0.

Flat and slant or V-type fracture modes

It has been shown that the onset and completion of transition from flat to slant mode of fatigue fracture occurs at specific valves of effective stress intensity range (Von Euw and others, 1982). It is reasonable to assume that the ratio $\tilde{W}p/t$ ($\tilde{W}p$ is cyclic plastic zone length ahead of the crack tip, t is thickness) is the controlling factor for fracture mode transition. It is ofcourse important to note that environment can also affect transition (Vogelesang, 1975). The critical values are possibly functions of the material, environment and frequency.

Thickness effect

The effect of thickness on crack growth rates arises from its effects on crack closure, crack extension mode transition and fracture toughness. Prior to onset of transition to slant mode, plane strain conditions will prevail. During transition, fracture mode is a composite of flat and shear. Hence, crack growth rate during transition will be given by

$$\frac{da}{dN} = \frac{A_{1g}\bar{t}_s(1-R_e)^{-m}(\Delta K_e - \Delta K_{th})^{p} + A_{2g}(1-\bar{t}_s)(1-2\nu)^{p}(1-\bar{R}_e)^{-m}(\Delta \bar{K}_e - \Delta \bar{K}_{th})^{p}}{[K_c^2 \bar{t}_s + K_{IC}^2(1-\bar{t}_s)] - K_{max}^2} \quad -- 12$$

where $\bar{t}_s$ is shear lip thickness expressed as a fraction of total thickness, $\Delta \bar{K}e$ is effective stress intensity range at mid thickness, ΔK_e is effective stress intensity range in the surface layers, Re and $\bar{R}e$ are

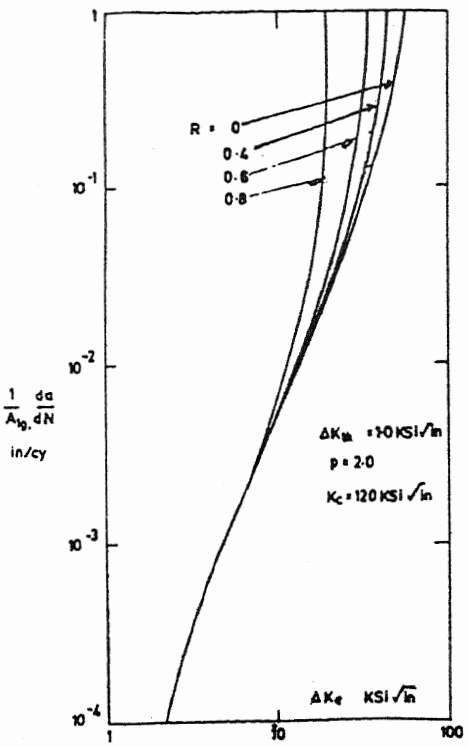

FIG 25

EFFECT OF STRESS RATIO R ON CRACK GROWTH RATE CURVE - TRENDS AS PREDICTED BY THEORY

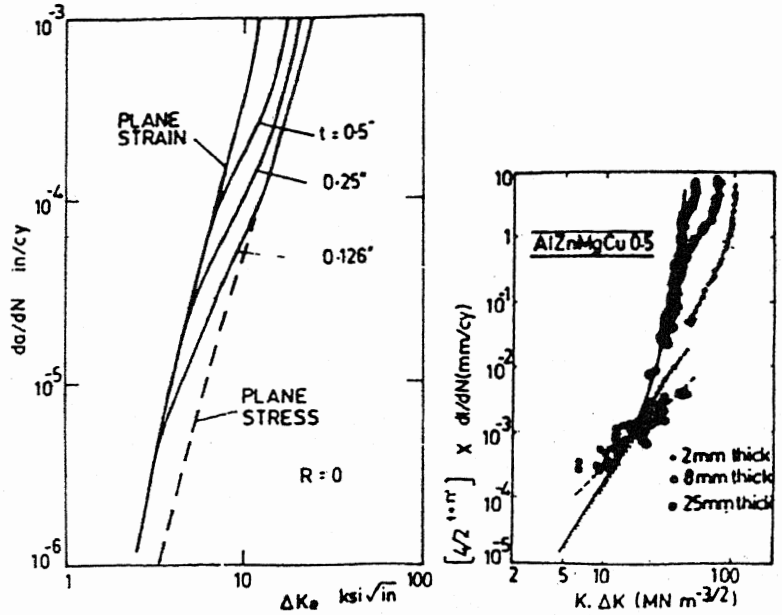

FIG 26 EFFECT OF THICKNESS ON CRACK GROWTH RATE CURVES - TRENDS AS PREDICTED BY THEORY COMPARED WITH EXPERIMENTAL RESULTS OF SCHWALBE (1979).

the effective stress ratios at surface and mid thickness regions respectively.

In the above equation, two separate values of ΔK_e and Re have been assumed in view of fractographic evidence (Sunder and Dash, 1982) showing that crack opening stress level at mid thickness can be significantly lower than that at the surface. For a range of thickness, the final fracture condition may be governed by fracture toughness values between K_c and K_{IC} and associated with a composite fracture mode. In such a situation, the ΔK_{cr} is governed by $K_c(t)$ which can be related to K_c, K_{IC} and the shear lip fraction at fracture, $\bar{t}_{sf}$ as

$$K_c(t) = K_{IC}^2 (1 - \bar{t}_{sf}) + K_c^2 \bar{t}_{sf} \qquad -- 13$$

The trends in the effect of thickness and crack growth rate, evaluated with some assumed values of constants in the growth rate equation are shown in Fig.26. They correlate well with experimental data obtained by Schwalbe (1979).

It is important to observe that at very high stress ratios, ΔK_e could exceed ΔK_e corresponding to Kmax = K_{IC} This condition is conducive to 'pop-in' crack extension. Fig.27 shows such conditions. It follows that 'pop-in' can occur even in relatively thin materials (t = 2 mm), provided the stress ratio is very high.

Non LEFM conditions

Non LEFM conditions can be taken into account in the crack growth rate expressions. Three situations need consideration. (i) - The monotonic plastic zone is comparable to crack length or net section. (ii) - Both monotonic and cyclic plastic zones are comparable to crack length and net section. (iii) - Gross yield. In (i), the growth rate equation can be modified using plastic zone corrected Kmax in the denominator. Similarly, in case of situation (ii), one can modify the growth rate relation using plastic zone correction for Kmax as well as ΔK_e. For situation (iii) one has to resort to EPFM concepts such as J integral. It is to be observed that the energy balance equation can be set up in terms of J integral since it represents energy release rate and also characterises the stress-strain fields at the crack tip in the EPFM range. The growth rate equation will take the form

$$\frac{da}{dN} = \frac{A \left(\sqrt{\Delta J_e . E}\right)^p (1 - R_e)^{-m}}{J_{cr} - J_{max}}$$

where ΔJ_e is the effective J integral range.

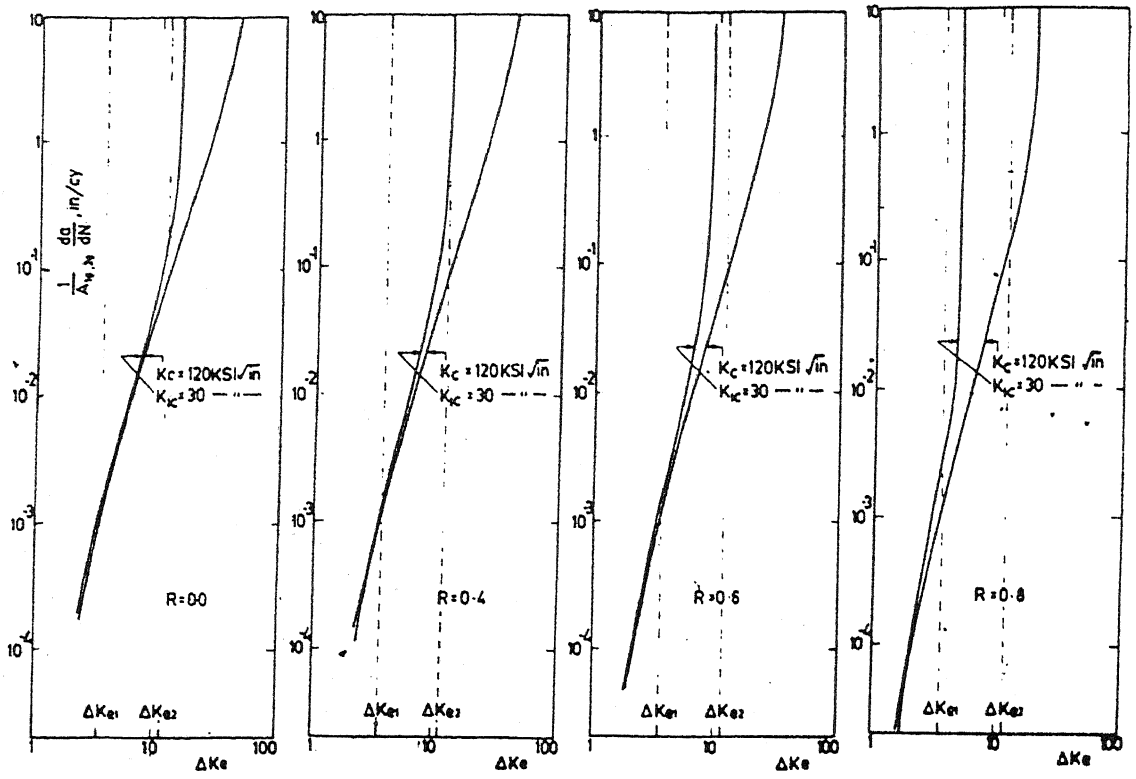

K_{max} = 37 Ksi$\sqrt{in}$ ≯ K_{IC}

Al-Zn-Mg Alloy t = 2mm

"POP-IN" CRACK EXTENSION

FIG 27 EFFECT OF STRESS RATIO ON CRACK GROWTH RATE CURVES FOR PLANE STRESS AND PLANE STRAIN INDICATING FRACTURE MODE TRANSITION POINTS AND POSSIBILITY OF "POP-IN" CRACK EXTENSION AT HIGH STRESS RATIOS

Correlation of test data with model

Fatigue crack growth data were generated under constant amplitude loading with stress ratio ranging from 0 to 0.85 on 1 and 5 mm thick Al-Cu-Mg alloy sheet material (Soviet D15AT) alloy). The tests were carried out on an INSTRON 1343 servohydraulic computer controlled testing machine. Software was developed for fully automated testing (Sunder, 1984). Figs. 28 and 29 show the crack growth rate data represented in formats corresponding to the Elber, Forman and proposed equation for crack growth rate. As evident from these figures, the proposed equation offers better correlation.

Environmental effects

The structure of the energy balance equation is such that it can be generalised to include environmental effects. An additional term on the righthand side, representing time dependent damage due to environment needs to be introduced. This has been discussed in detail elsewhere (Raju 1980). It can be shown that superposition and process competition models of environment assisted fatigue crack growth can be obtained as special cases using the generalised energy balance equation. In the setting up of the energy balance equation and in the subsequent derivation of the crack growth rate relation, the concepts of damage, energy balance and crack closure are closely involved in a unified manner.

Variable amplitude loading

The unified model of fatigue crack growth described above can be easily extended to deal with crack growth under complex load sequences like flight-by-flight loading, since the basic parameter that control interaction effects such crack closure is inherent in the model. Since the model is based on hysteresis energy, rainflow cycle counting for discerning load cycles for complex load sequences is appropriate to the model. The applicability of rainflow cycle counting technique to fatigue crack growth analysis under complex load sequences has been established by Sunder and co-workers (1984) using a novel fractographic technique.

General Remarks

The unified approach to modelling fatigue crack growth essentially combines the concepts of damage, energy balance and the phenomenon of crack closure. The model has been shown to account for the effects of a number of parameters, in a logical manner, on crack growth rates. The model is essentially continuum mechanics based involving continuum parameters and as such any efforts towards extending the model to account for microstructural parameters may begin with the relationship between continuum parameters and microstructure. An obvious approach to consideration of microstructure parameter and fracture modes or mechanisms is to observe that the hysteresis energy absorbed can produce inhomogenous damage leading to the situation where energy required for a specific mechanism to operate becomes minimal. In its present form the model cannot be directly applied to mixed mode fatigue crack growth like under combined K_I amd K_{II} conditions. This will require recognition of the fact that energy release rate feeding to the process of crack extension is dependent on the angle of crack extension. Also the hysteresis energy absorbed and the damage resulting

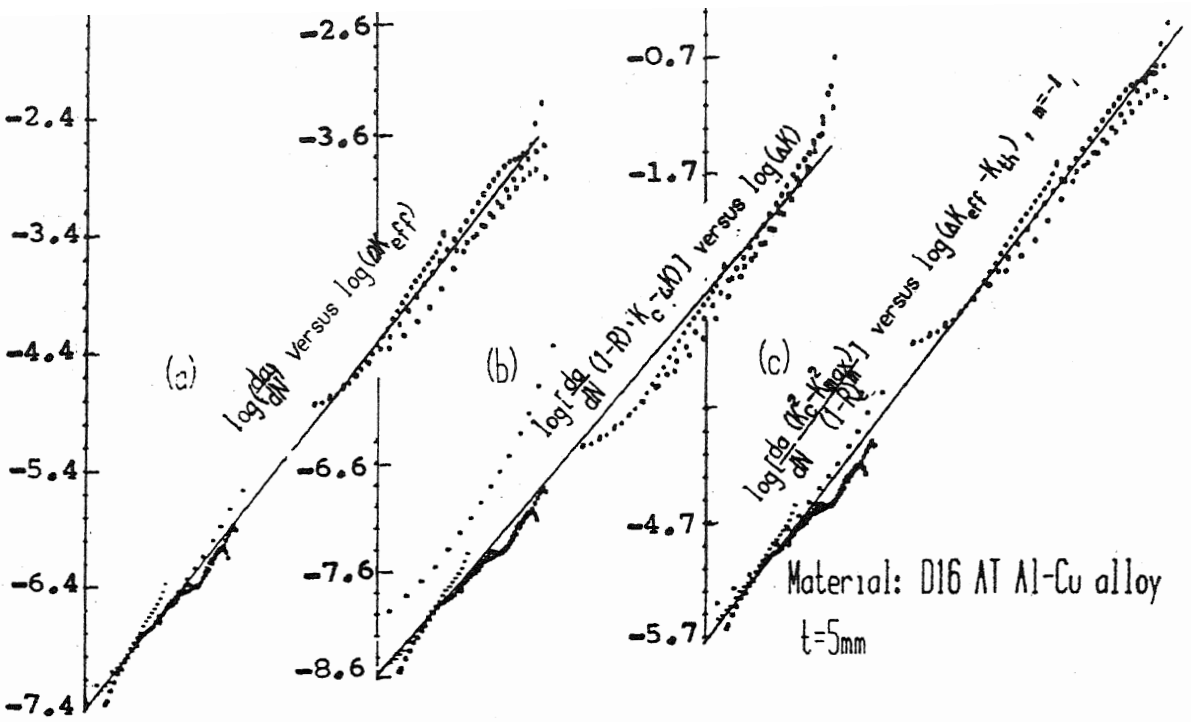

FIG 28 CORRELATION OF CRACK GROWTH RATE DATA ON 5mm THICK Al-Cu ALLOY WITH (a) FORMAN (b) ELBER (c) PROPOSED CRACK GROWTH RATE RELATIONS

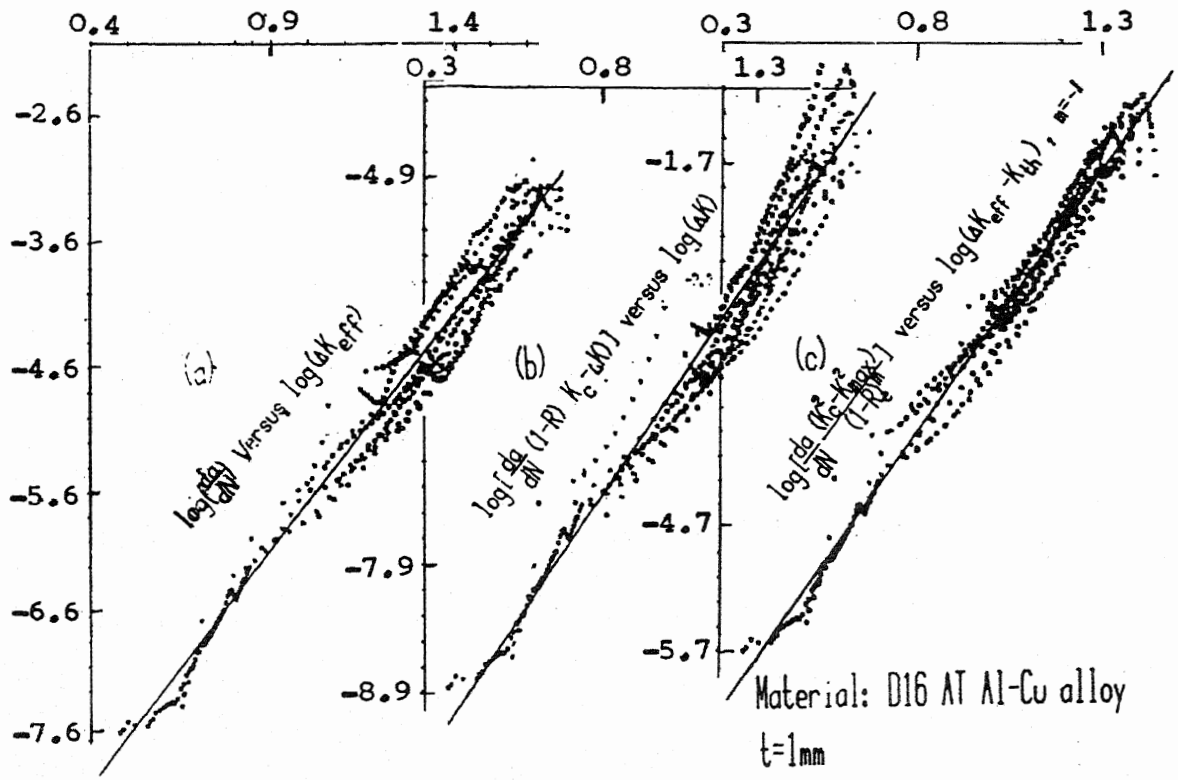

FIG 29 CORRELATION OF CRACK GROWTH RATE DATA ON 1mm THICK Al-Cu-ALLOY WITH (a) FORMAN (b) ELBER (c) PROPOSED CRACK GROWTH RATE RELATIONS.

from it could be function of the mode I and mode II components of the crack tip stress field.

B. EXPERIMENTAL STUDIES

Experimental studies have been entirely in the area of fatigue crack growth with perticular emphasis on variable amplitude loading and interaction effects. Electron fractography has been extensively used in all the studies carried out. The following sections describe the studies carried out in some detail.

(B.1) Studies on fatigue crack closure and its measurement through electron microscopy

(Sunder and Dash 1982)

The phenomenon of fatigue crack closure can explain the influence of a number of factors on fatigue crack growth. These include stress ratio, material thickness, load and environmental history. Many experimental techniques are available for measurement of crack opening stress. They involve monitoring a certain diagnostic parameter (e.g. AC/DC potential drop, crack opening displacement, ultrasonic flux etc.) whose variation is related to the interaction between applied load and closure of the fatigue crack due to compressive residual stresses in the front and in the wake of the fatigue crack. Data from the literature show a lack of consistency in crack opening stress estimated using these techniques.

A technique has been developed for accurate estimation of crack opening stress. This method involves electron fractography of the fatigue fracture surface obtained under specially designed fatigue load sequences. Experiments were conducted on 5 mm thick, 70 mm wide single edge notch specimens of an Al-Cu-alloy known to be conducive to the formation of fatigue striations. Typical results obtained in this study appear in Fig.30. The load sequence is with constant maximum stress and stepwise cycle-by-cycle variation in minimum stress (Fig.30 top). The load signal for this sequence was generated by a digital computer. If repetitive blocks of such a load sequence are applied, a stable crack opening stress will develop which will depend on the maximum and lowest minimum stress in the block. According to the crack closure concept all the load cycles with minimum stress lower than the crack opening stress will have the same effective stress range. As a result one will find a group of equally spaced striations associated with these load cycles. By correlating the number of such striations with the load sequence used the crack opening stress is directly determined.

The upper and lower fractographs in Fig.30 correspond respectively, to the area close to specimen surface and close to the mid thickness. From the upper photo we can conclude that the crack opening stress level is equal to the minimum stress in the third and thirteenth (first and last equally spaced striation) load cycles. Similarly it follows from the lower photo that the crack opening

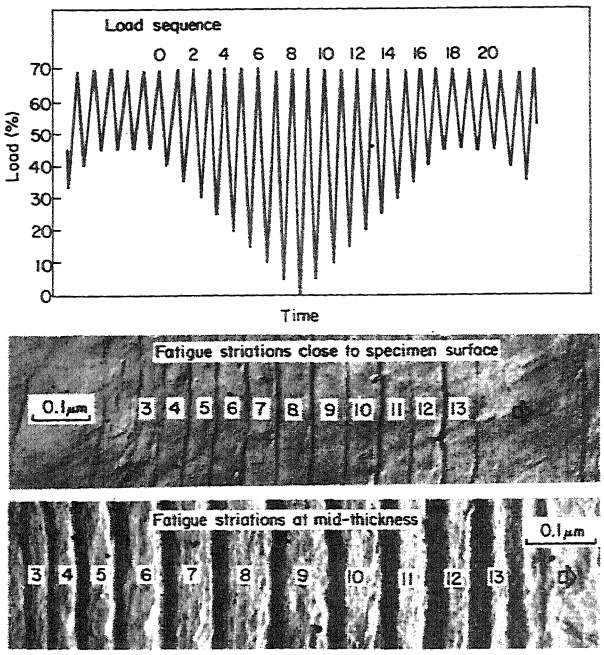

Load sequence and fatigue striations close to specimen surface (upper photo) and at mid-thickness (lower photo) for specimen D ($t = 5$ mm)

$$\left(\frac{\overline{da}}{dN}\right)_R = \frac{(da/dN)_R}{(da/dN)_0} = \frac{[K_{max} - \max(K_{min}, K_{op})]^m}{[K_{max} - K_{op}]^m}$$

For zero stress ratio,

$$K_{op} = (1 - k_1)K_{max} =$$

Then,

$$\left(\frac{\overline{da}}{dN}\right)_R = \left[\frac{1 - \max(R, 1 - k_1)}{k_1}\right]^m \qquad (11)$$

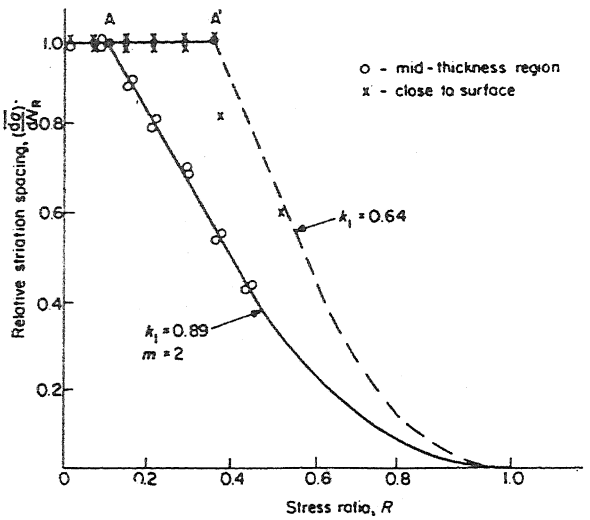

Relative striation spacing close to surface and at mid-thickness (curves according to Equation (11)). k_1 values from intersection points A and A'. Slope m was selected to suit data for mid-thickness region

FIG 30 FRACTOGRAPHIC OBSERVATION OF CRACK OPENING STRESS CLOSE TO SURFACE AND AT MID THICKNESS.

stress level at mid thickness is equal to the minimum stress in cycles 6 and 10. These results indicate that the crack opening stress level is considerably greater at the specimen surface as compared to the mid thickness region. This is further made clear in the plot of relative striation spacing (normalised with respect to maximum striation spacing) versus stress ratio R of the load cycles in a block shown in Fig.30. It is to be appreciated that this fractographic method provides a simple procedure for determination of crack opening stress and its variation through the thickness which is not possible by other methods.

(B.2) Binary coded event registration on fatigue fracture surfaces (Sunder, 1982, 1984)

The fatigue fracture surface contains a permanent "record" of the cycle-by-cycle growth of the fatigue crack. With the assistance of electron fractography this information can be analysed to determine load history leading to failure (failure analysis) and the effect of material microstructure, load sequence, frequency, environment and other factors on fatigue crack growth behaviour.

In the case of laboratory simulated fatigue failures, the objective is to study the nature and width of fatigue striations induced by a specific variation in fatigue load, frequency, environment etc. A major problem in such studies is the identification of the precise region (micro region) of interest at very high magnifications. The problem is further aggravated if part through or embedded cracks are being investigated or if transmission electron microscopy is used to study replicas. In the case of the former the crack front geometry cannot be closely monitored during the test as a function applied load cycles. In the case of the latter the replica contour is liable to be distorted during preparations rendering it almost impossible to associate it with any location on the fracture surface.

Exploratory studies carried out show that load sequences can be designed to leave "binary coded signatures" in the form of pre-programmed fatigue striation patterns on the fracture surface. Such load sequences can be used to register events during fatigue tests and can be later identified during electron fractographic examination of the fracture surface. Fig.31 and 32 show typical binary coded load sequences and associated striation patterns. These load sequences were used in computer controlled crack growth tests on SEN specimen made from an Al-Cu alloy of 5 mm thickness. The load sequence in Fig.31 contains two parts. The sequence of load cycles in the first part is used to estimate crack opening stress level. The load sequence in the second part represents a binary number. It consists of three different maximum stress levels; the highest one represents '1', the intermediate level a '0' while the lowest level is used to generate markers for subsequent identification on the fracture surface. In this sequence, the binary number represents the number of the current block (562) of fatigue loads.

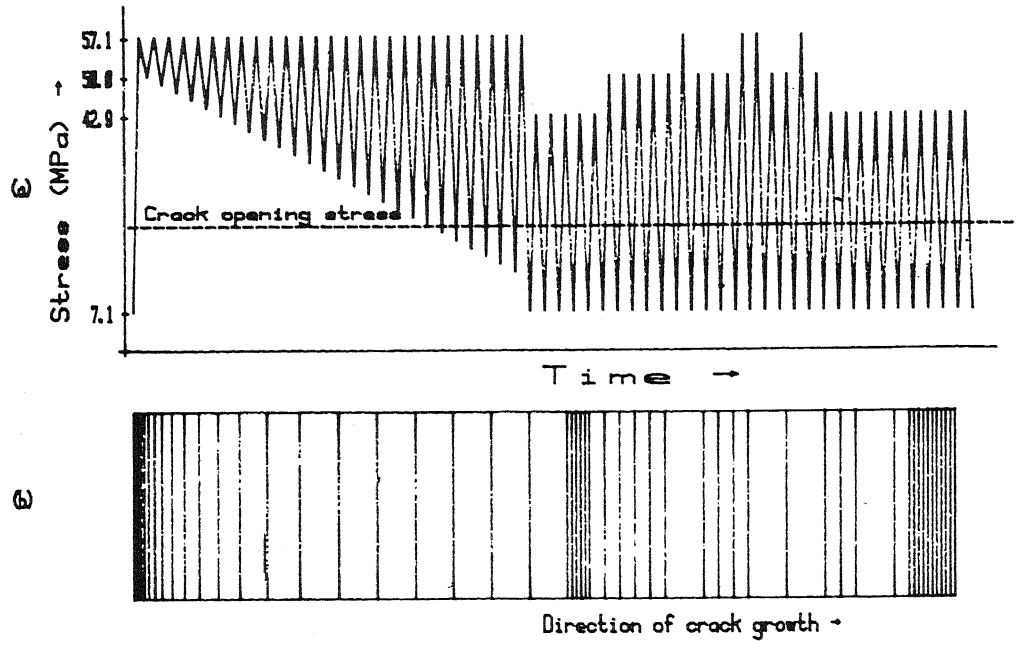

Load sequence and expected striation pattern in Test C

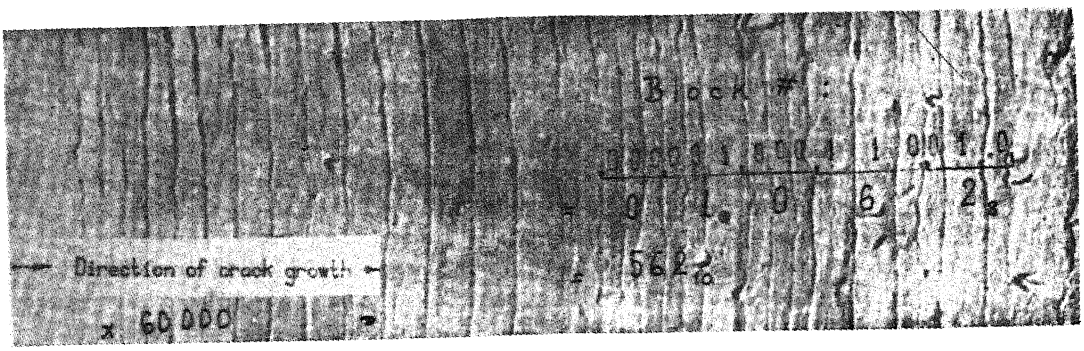

Typical fractograph from Test C. Striation pattern represents #562

FIG 31 LOAD SEQUENCE FOR CRACK CLOSURE MEASUREMENT AND BINARY CODED EVENT REGISTRATION ALONG WITH ASSOCIATED STRIATION PATTERN - BINARY CODED EVENT IS LOADING BLOCK NUMBER 562.

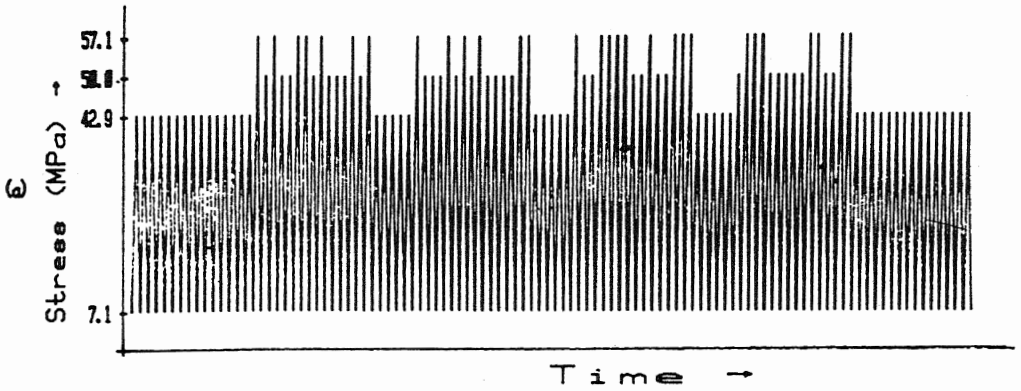

(a)

(b)

Load sequence and expected striation pattern

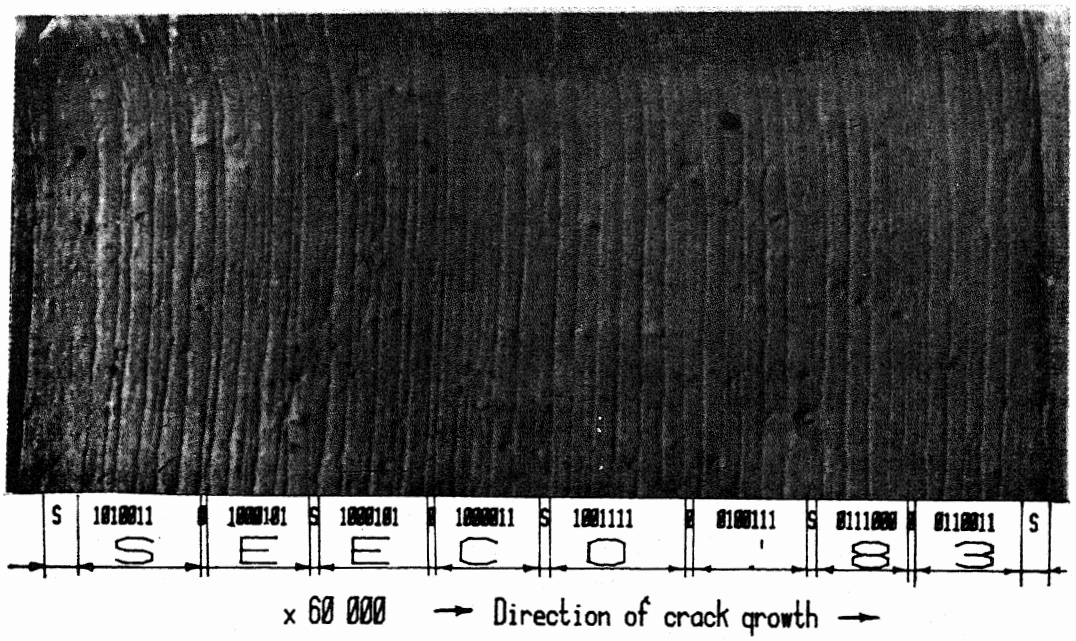

Typical fractograph from test D showing striation pattern representing the ASCII encoded string "SEECO'83"

FIG.32 BINARY CODED REGISTRATION OF " SEECO-83 " ON FRACTURE SURFACE
("SEECO-83" - SOCIETY OF ENVIRONMENTAL ENGINEERS CONFERENCE 1983).

The expected striation pattern computed from constant amplitude crack growth data appears below the load sequence. The fractograph (Fig.31 bottom) corresponds precisely to the expected pattern. From this photograph we can not only estimate the precise crack opening stress level but also the number of the block of loads (the event) for which it was measured. The results in Fig.32 indicate the reliability of the proposed technique for event registration. In this test the ASCII coded load sequence representing the character string "SEECO'83" produced an extremely clear striation pattern (Fig.32 bottom) ("SEECO'83" is the logo of the society of Engironmental Engineers Conference on "Digital Techniques in fatigue" London, March 28-30, 1983 at which this work was presented). This indicates that fairly complex striation patterns can be reproduced with clarity provided, of course, the material is conducive to striation formation and the load levels are judiciously selected.

This technique of event registration is being advantageously used in an on-going study on growth of short part-through cracks initiated at notches. The objective is to study crack growth behaviour including growth rates, crack front geometry and crack closure variation along the crack front. The studies cover both constant and variable amplitude loading.

B.3. Studies on fatigue crack growth under variable amplitude loading

Interesting experimental studies have been carried out on fatigue crack growth under variable amplitude loading (Sunder and coworkers 1983, 1984, Sunder 1984). These studies are described after a brief review of fatigue crack growth under variable amplitude loading, analytical models and prediction techniques.

Engineering structures are subject to a complex load environment which is random in nature. Fatigue crack propagation under such conditions is of considerable interest, particularly in the design of fail-safe, damage tolerant structures. Early studies of crack growth under simple variable amplitude loading (Schijve, 1960, Hudson and Hardrath, 1961) showed that application of overloads or reduction in load level introduced a noticeable retardation in crack growth rate. The practical implications of these observations triggered exhaustive studies under various load sequences. A detailed review of literature on the subject was made by Schijve (1976, 1980) with particular reference to aircraft materials and load spectra. A brief summary of general observations is given below. This is followed by a discussion on mechanisms contributing to load interaction effects. A number of available models for crack growth prediction are described. The significance of fatigue cycle counting in life estimates is explained.

Load interaction effects under simple variable amplitude loading

Positive overloads introduce noticeable delay, even arrest, in crack growth (von Evw and others, 1972). Fractographic studies revealed the phenomenon of delayed retardation after overloads

(McMillan and Hertzberg, 1968). They also show that crack extension during the overload itself is much greater than what one might expect on the basis of constant amplitude data (von Euw and others 1972). Introduction of even a large number of intermediate load cycles of small magnitude (not contributing to crack growth) after an overload does not reduce delay, indicating that delay effects are crack extension dependent rather than cycle dependent (Potter, 1972). Delay increases with magnitude of overload, application of multiple overloads (Hudson and Raju, 1970), and by repetition of overloads after some crack extension (Mills and Hertzberg, 1975, 1976). Dwell introduced at high load increases delay (Jonas and Wei, 1971). On the other hand, a heat soak after an overload can reduce or even eliminate retardation effects (Raju and others, 1972).

The application of periodic underloads is known to have little effect on crack growth under constant amplitude loading (Hsu and Lassiter, 1974). Their application prior to a positive overload also is not very damaging. However negative overloads applied immediately after a positive overload can reduce subsequent delay (Schijve and others, 1961; Stephens, 1977).

A Hi-Lo stepwise change in load level introduces immediate delay or even crack arrest (Hudson and Raju, 1970). It is not easy to discern any acceleration effect after a Lo-Hi transition, because of the rather high baseline crack growth rate. However, evidence is available (Mathews and Baratta, 1971) indicating some acceleration after such a change.

Service load spectra essentially represent complex combinations of the simple load variations discussed above. It is only natural therefore that load spectrum effects on crack growth are also similar. Extensive studies at NLR on 2024-T3 and 7075-T6 alloy sheet material under a transport wing load spectrum (Schijve and others, 1968, 1972; Schijve, 1973) showed that:

1. On the whole, crack extension in larger cycles is greater and in smaller cycles less, than what one would expect from constant amplitude data. Overall, crack growth rates are much less than linear damage accumulation estimates.
2. Randomization of the load sequence instead of applying large equivalent programmed blocks increases crack growth rates by upto a factor of 3. However, resequencing of loads within individual flights (short programmed blocks) is of no consequence.
3. Introduction of the Ground-Air-Ground cycle (by including the associated compressive load between flights) can double the crack growth rate.
4. Increase of load truncation level causes a dramatic increase in crack propagation llife.

5. Variation in load frequency over upto two orders has no effect on the crack growth process.

It must be noted that most of the observations listed above pertain to relatively low strength, high toughness thin sheet materials tested in laboratory conditions. Such materials show greater sensitivity to load sequence in view of plasticity induced effects at the crack tip. They are susceptible not only to increased retardation (due to overloads) but also to adverse effects of underloads (Stephens, 1977). Thicker materials show greater constraint to plastic deformation. Studies on 2024-T3 material (Schijve and others, 1976) show that retardation effects in thicker material (t = 10 mm) are negligible as opposed to those in thin material (t = 2 mm). The same study also showed that retardation is not affected by environment apart from the general increase in growth rates also observed under constant amplitude loading.

Data in the literature indicate a mean stress effect on crack growth rate under spectrum loading (Schijve, 1972). These will be discussed later in the context of prediction models.

Mechanisms of load interaction

Generalisation of fatigue crack growth data is based on the assumption that similar crack tip conditions will give similar crack growth rates. This also forms the basis for a number of load interaction models which attempt to explain the violation of similarity at the crack tip under variable amplitude loading. The suggested mechanisms include:

1. Crack tip blunting-resharpening under the influence of changing load amplitude (Christensen, 1959). Assuming this to be a predominant mechanism, one would expect delay/acceleration to be cycle dependent - experience shows rather, that they are crack extension dependent.
2. Strain hardening/softening in the crack tip area. The significance of this mechanism is placed in doubt by observations (Mills and others, 1977) that retardation behaviour under overloads is qualitatively similar in 2024-T3 (a cyclic strain hardening material) and A514F steel (whcih exhibits cyclic strain softening).
3. Crack branching. A fatigue crack can branch into two or deflect under the influence of a tensile overload (Suresh, 1982). Delay effects follow due to reduction in K at deflected/branched crack tips with distribution of local displacements over two close cracks and also due to the change in plane of the crack. The latter also affects the mode of crack extension. It must be pointed out that crack branching/deflection occurs only after very large overloads and under predominantly plane stress conditions. Further, this mechanism cannot explain most other interaction effects including that of heat soak after overloads.
4. Residual stresses at the crack tip left by overloads/underloads. This can explain many observations on delay/acceleration.
5. Fatigue crack closure due to interaction of residual deformations ahead and in the wake of the crack tip (Elber,1970).

Crack closure can also be induced at near threshold conditions by the formation of oxide layers on the fracture surface (Suresh and others, 1981). Fatigue crack closure is currently the most widely used mechanism in various models for crack growth prediction.

6. Crack front incompatibility. Shear (slant) mode cracking is associated with high stress intensity while tensile (flat) mode crack extension is associated with smaller load cycles. Under variable amplitude loading, load interaction effects can arise due to incompatibility in crack front orientation (schijve, 1973, 1980).

Models for prediction of crack propagation under variable amplitude loading are extremely important from the viewpoint of fail-safe, damage tolerant design. Numerous methods are proposed in the literature. These are based either on one of the load interaction mechanisms listed above or on statistics of crack growth under variable amplitude loading. Many of the models were developed to describe delay effects under simple variable amplitude loading. These are only of academic interest and will not be discussed here.

Crack tip blunting-resharpening

Christensen (1959) related retardation and acceleration effects to different crack tip stress concentration as affected by load range. Later, McMillan and Pelloux (1970) used a model based on this concept to explain fractographic observations of fatigue crack growth in 2024-T3 under repeated blocks of programmed and pseudo-random loading. It must be pointed out that these were short blocks with multiple load levels. Under such conditions, the crack tip area experiences a rather stable plastic zone size and crack extension in each cycle will be affected by current stress intensity excursions rather than long term load history. This model would be unable to explain crack extension dependent effects of retardation and acceleration one observes after overloads, etc.

Residual stress models

Wheeler (1972) proposed a model which assumes that crack growth rate is reduced by a retardation factor, Cr while the crack propagates through the plastic zone left behind by a prior overload. Cr varies exponentially from a fraction of one to unity in inverse proportion to the distance between the boundary of the current monotonic plastic zone and that of the overload plastic zone. The exponent in the power relation cannot be determined analytically. It is usually selected to fit experimental data and has been found to remain fairly constant for a given type of spectrum loading (Keays, 1972). The model lacks a sound physical basis in view of its inability to explain accelerated crack growth and delayed retardation.

The Willenborg model (1971) assumes retardation to be associated with a certain effective crack tip stress ratio (less than the remotely applied R) as affected by residual stresses in the overload plastic zone area. Unlike the wheeler model, it does not require any empirical constants to describe retardation, apart from baseline constant amplitude data as affected by R. Its limitations are similar to those of the Wheeler

model - it is insensitive to the effect of compressive stresses. This model was subsequently modified to account for crack arrest (Johnson and others, 1978) and the adverse effect of compressive loads (Johnson, 1981). The latest version referred to as a "Multi-Parameter Yield Zone Model" has four additional empirical constants. These contribute to improved prediction accuracy.

Crack closure model

Experimental studies of crack growth under simple variable amplitude loading (Elber, 1971) as well as spectrum loading (Elber, 1976) show an excellent correlation between observed results with measured values of crack closure stress and associated effective stress intensity. The phenomenon of crack closure has in recent years been subject to extensive theoretical and experimental studies. Numerous empirical (Bell and Wolfman, 1976; Sunder 1978, 1979b) and analytical (Newman, 1981; de Koning, 1980) models have been suggested to estimate crack closure stress and associated crack growth rates under complex load sequences.

It is logical to expect that fatigue crack closure is the predominant load interaction mechanism in thin materials. After all, crack growth rate is a power function of effective stress intensity range - which in turn varies linearly with crack opening stress level. Other load interaction mechanisms can only have a secondary influence on crack growth rate.

A modified Dugdale model was developed and successfully used by Newman (1981) in analytical studies of crack growth under a variety of load sequences. Life predictions for 6.35 mm thick 2219-T851 aluminium alloy sheet material under various spectrum loading conditions were very close to experimentally obtained values. An important element of the Newman model is its ability to account for thickness effect on crack closure. However, it must be pointed out that even the Newman model requires empirical data on stress state (thickness) effects on crack closure. This underscores the importance of experimental studies of the closure phenomenon.

Under spectrum loading, crack closure stress remains more or less constant (Elber, 1976) and is a function of the major spectrum variables. Schijve (1980) showed that reasonably accurate estimates of crack propagation life can be made assuming Sop to be controlled by the maximum and minimum stress levels in the spectrum. A regression model was developed (Sunder, 1978, 1979a) to approximate Sop as a function of spectrum truncation level and spectrum severity (rms amplitude). It was checked out using available data for 2024-T3 and 7075-T6 obtained at NLR (Schijve and others, 1968, 1972). This model permits accurate interpolation of crack growth rates for a given material and load spectrum over a wide range of mean stress, load truncation and omission levels. It can assist in minimizing the volume of testing required to evaluate fatigue performance for a new material or spectrum. Moreover, as Sop is assumed to be constant, cycle-by-cycle crack growth estimates can be avoided by resorting to an equivalent stress or Miner type of calculation, thereby reducing computer time.

Characteristic K approach

Barsom (1976) corrrelated variable amplitude crack growth rate data with constant amplitude data by plotting da/dN versus Krms. Hudson (1981) later used this technique to predict crack growth under flight-by-flight loading. His prediction ratios for 6.35 mm thick 2219-T851 alloy sheet material ranged from 0.82 to 2.13 depending on the spectrum and stress level. This approach can be valid for narrow band type of loading, particularly, with a large tensile mean stress offset, where load interaction is less. A more realistic approach would be to correlate da/dN with a characteristic K for the given spectrum of interest. Ignoring dK/da effects and considering the spectrum to be of short duration, similarity at the crack tip is ensured by similar characteristic K. Tests at a few mean stress levels under aircraft manouevre spectrum loading showed reasonable correlation between da/dN and Km (Wanhill, 1978).

The characteristic K approach appears to be attractive from the view point of engineering application - the designer is provided with a single curve which by integration yields crack propagation life. Unfortunately, this statement cannot be generalised. Even for a given load spectrum, material and specimen geometry, da/dN versus Km curves for different mean stress, Sm, do not fall into a single scatter band (Schijve and others, 1972). There appears to be an order of magnitude variation in da/dN at a given Km, depending on Sm. Schijve attributed this observation to the possible influence of dK/da. This appears to be unusual in view of the absence of dK/da effects under constant amplitude loading.

Of the various load interaction models, the crack closure model appears to be the most versatile. It explains most observations including dK/da effect under spectrum loading. However, a few other load interaction mechanisms (e.g. crack front incompatibility) can also "swing into action" to produce anamolous results. Future work should therefore be directed towards the development of multi-mechanism models for prediction purposes. Finally, cycle-by-cycle estimates take up more computer time than calculations of average crack growth rates. In the process, no noticeable improvement in prediction accuracy is often achieved. Therefore, cycle-by-cycle estimates may be avoided wherever spectrum duration is so short that truncation level loads repeat more than once within a plastic zone.

The primary objective of most crack growth prediction technqiues has been to simulate interaction effects under complex load sequences and superimpose them on the baseline constant amplitude properties of the material. In the process, the vital question of fatigue cycle counting is often totally ignored. Unlike a constant amplitude sequence, random peaks and troughs seldom show discernible (closed) fatigue cycles. This invalidates direct application of baseline da/dN versus K data. Obviously, cycle counting should form an integral part of any crack growth analysis for random loading. A number of techniques are available for analysis of random load history (de Jonge, 1982). The question now arises as to which cycle counting technique to use in fatigue crack growth analysis. The Rainflow cycle counting technique has a physical basis for notch root fatigue studies in view of its relationship with the formation of closed hysteresis loops in the local stress strain diagram. The moving fatigue crack tip however complicates the situation.

It is evident that any prediction technique of fatigue crack growth under random loading should necessarily involve an appropriate cycle counting technique. The unified model based on hysteresis energy presented earlier indicates that the rainflow cycle counting technique is appropriate. An interesting experimental study has been carried out to establish the applicability of rain flow cycle counting in fatigue crack growth under random loading. Carefully planned fatigue crack growth tests have been carried out, with K-control, on edge crack specimen under fighter aircraft spectrum loading to study the effect of dK/da on crack growth rates. These studies are described in some detail in the following section.

(B.3.1) Cycle counting technique for fatigue crack propagation
(Sunder and cowrokers, 1983, 1984)

Fatigue analysis of engineering structures is complicated by the variable and often random nature of service loads. Baseline fatigue data are usually obtained under conditions of constant stress amplitude loading. During fatigue analysis, these have to be extrapolated to service load environment.

The sequence of 'g' loads acting on a typical combat aircraft during one flight is shown in Fig.13. An important aspect of fatigue analysis is the process of cycle counting to identify "complete" load cycles from a given random sequence of peaks and troughs. A number of cycle counting technqiues for analyses of random loads are currently available. Of these, the most modern and meaningful is the so called 'Rain-flow' cycle counting technique. This technique is supported by a physical basis the closing of stress-strain hysteresis loops formed by the load cycles being counted. Obviously this technique can be considered most appropriate for analysis leading to estimates of crack initiation life at notch root or at the root of stress concentrations. However the use of the same cycle counting technique over the crack growth stage requires further considerations. In this stage of the fatigue process, we have to deal with a moving crack tip influenced by a "truncated" load history due to crack closure.

An investigation was recently carried out to study the validity of the rainflow cycle counting technique for the fatigue crack growth process. For this purpose a fatigue crack was grown under a specially designed load sequence on a computer controlled fatigue testing machine. The basis of the load sequences will be clear from the peak-trough sequence shown in Fig.33. These are divided into four segments A, B, C and D. As per the Rainflow technique, segments A and B are identical in damaging power. Each has two inner cycles (A1-A2, A3-A4), (B2-B3, B4-B5) and an outer cycle (A0-A5-A6), (B0-B1-D0). Cycle C (A6-C1-B0) is identical to the counted outer cycles while (D2-D3-D4), (D6-D7-D8) are identical to the two counted inner cycles each in A and B. If a fatigue crack is grown under repeated blocks similar to the one in Fig.33, using a material and stress levels conducive to the formation of fatigue striations, the validity of the Rainflow cycle counting technique can be examined on a quantitative basis through electron fractography of the fatigue fracture surface. Tests were carried out using seven

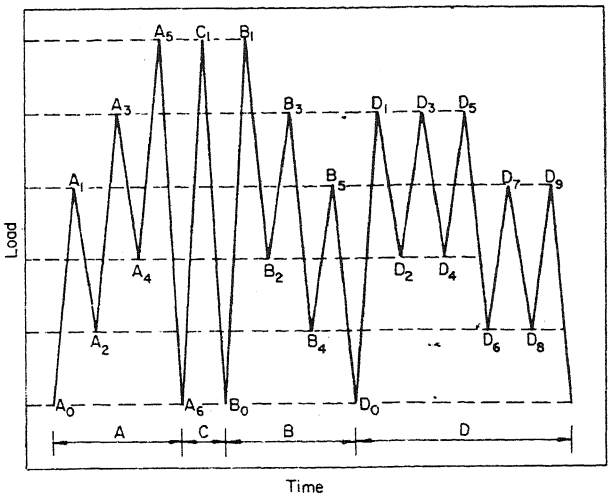

Fig.33 LOAD SEQUENCE DESIGNED TO VALIDATE CYCLE COUNTING TECHNIQUE

different load sequences built around the one in Fig.33. In these sequences, the number of inner cycles as well as their magnitude were varied. So was the minimum stress to study possible crack closure effects (inner cycles below closure stress can get 'eclipsed'.

The cycle step size in segment D was extended to between 25 and 100 cycles, depending on the counted stress range of the inner cycles. This ensured a measurable crack extension over the entire step. Crack extension due to individual cycles in D was estimated by dividing total extension in D by step size. A typical striation pattern appears in Fig.34 along with the load sequence and digitally processed fractograph. For Rainflow cycle counting to be valid, growth in segments A and B should be equal. In addition, 1/3rd the growth increment in A or B should be equal to 1/4th the increment in C plus 1/25th increment in D. The increment Do is due to the stress excursion from the minimum stress in segment B to the maximum stress in D. Fig.35 shows the seven different load sequences used in tests along with the equivalent striation patterns obtained by computer analysis of fractographs. Also shown in the figure are the results of fractographic analysis. The results of this study strongly support the use of Rainflow cycle counting to crack growth analysis. They also point to large errors that may occur if range count method is used. Range counting is consistent with COD based models.

(B.3.2)<u>Fatigue crack growth under fighter aircraft spectrum loading</u>

(Sunder 1984)

Fatigue crack growth data obtained under flight simulation loading, with a wide range of mean stress levels do not fall into a single scatter band when plotted against a characteristic K like mean stress intensity, K_m. As mentioned earlier, this has been attributed to the possible influence of dK/da (Sunder 1984). A study has been carried out on fatigue crack growth in 1 and 5 mm thick D16AT. Al-Cu-alloy sheet material under stress and K-controlled flight-

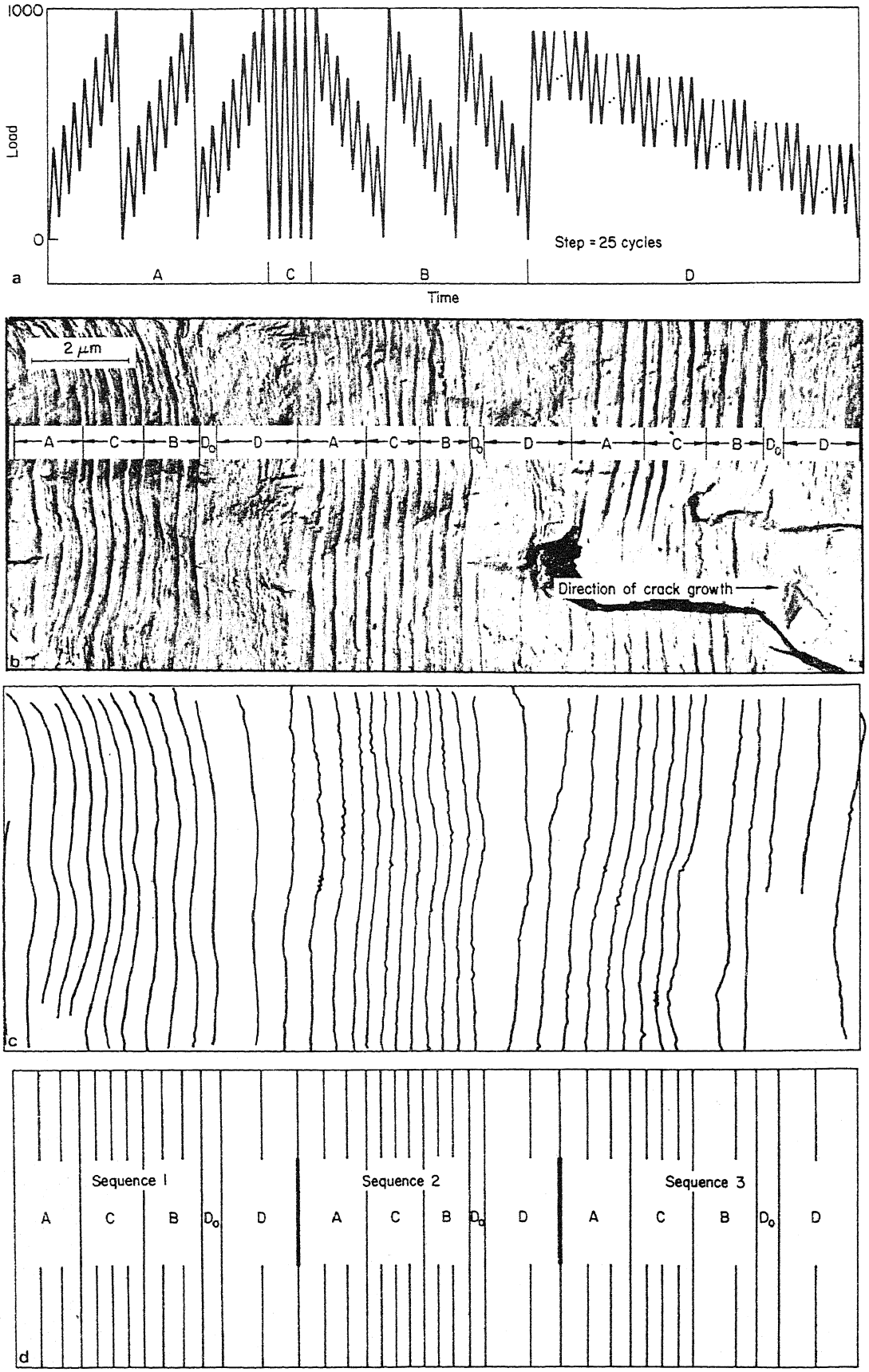

FIG 34 ANALYSIS OF FRACTOGRAPH OBTAINED UNDER LOAD SEQUENCE 2, (a) LOAD SEQUENCE (ONE BLOCK), (b) FRACTOGRAPH (COVERS THREE BLOCKS OF LOADS), (c) DIGITISED STRIATION PATTERN IMAGE, (d) EQUIVALENT STRIATION PATTERN COMPUTED.

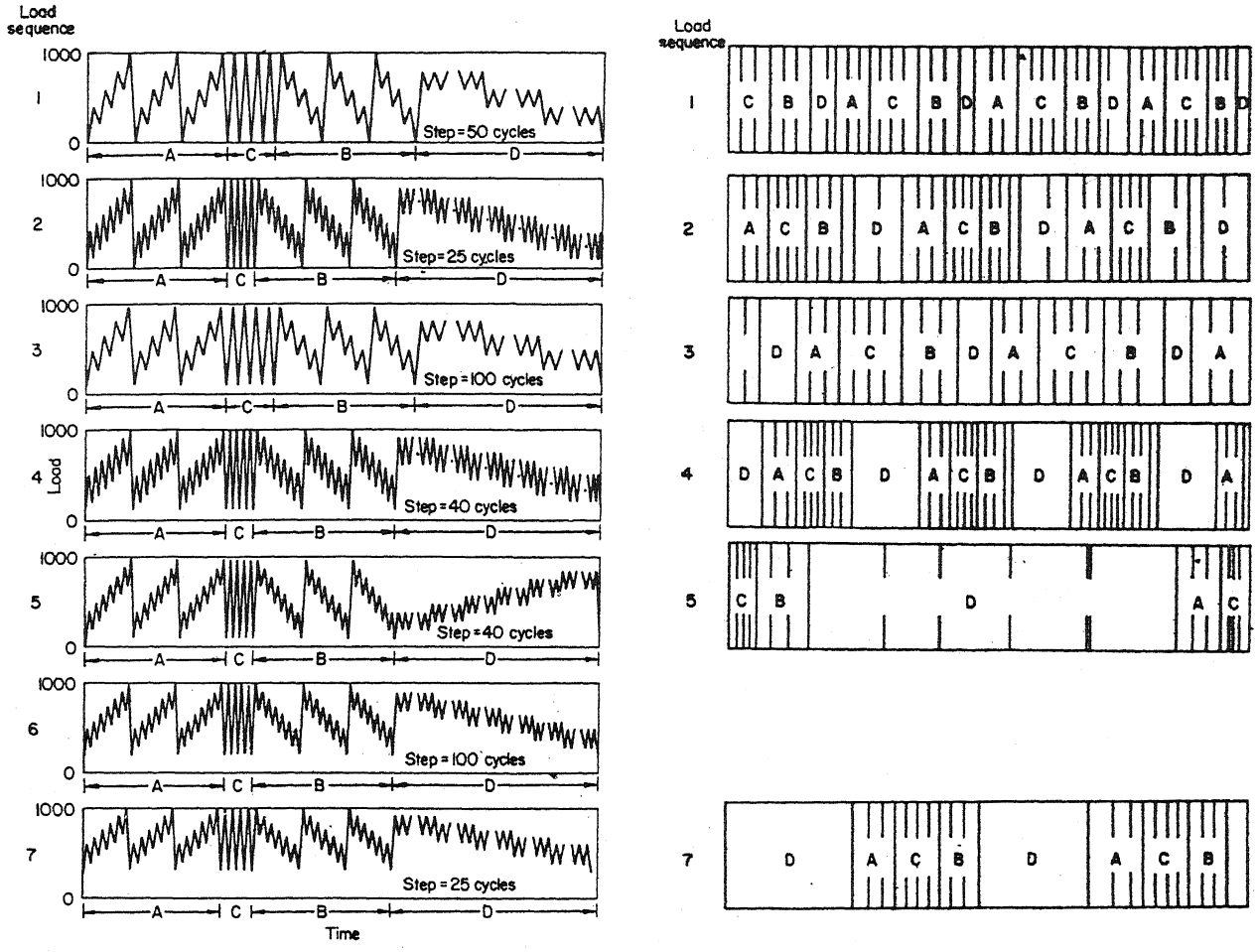

Sequence	Min load	Lowest peak	No of interr	Step size	A	B	0.5 (A + B)	C	D	C + D	Error A	Error B	Error (A + B)	Error (Range)
						(from striation spacings on fractographs)								
1	2	3	4	5	6	7	8	9	10	11	12	13	14	15
1	0	400	3	50	100	97.66	98.83	95.77	3.23	99.01	0.99	−1.18	−0.18	−229
2	0	400	6	25	100	82.68	91.34	67.01	14.77	81.78	18.22	0.9	9.56	−156
3	100	500	3	100	100	112.48	106.23	108.55	1.63	110.18	−10.18	2.29	−3.95	−140
4	100	500	6	40	100	91.36	95.68	65.25	17.05	82.29	17.7	9.07	13.38	−133
5	100	400	6	40	100	116.37	108.18	48.00	60.20	108.20	−18.20	8.17	−0.02	−115
6	200	500	6	100	100	(Excluded from analysis due to poor quality of fractographs)								−332
7	300	600	5	25	100	84.73	92.37	72.52	23.84	96.36	3.64	−11.63	−3.99	−432

Columns:

1. Load sequence number
2. Minimum load in block, L_{min} (maximum load = 1000 units)
3. Load level at lowest peak, L^*
4. Number of interruptions (inner cycles) in one outer cycle of A or B, n
5. Number of cycles in each step of segment D
6. Crack extension in one set of segment A (taken as reference and equal to 100%)
7. Crack extension in one set of segment B (%)
8. Average crack extension in one set each of segments A and B (%)
9. Crack extension in one cycle of segment C (%)
10. Cumulative crack extension due to one cycle from each of the steps in segment D (%)
11. Rainflow counted crack extension for A, B from fractograph (%)
12. Difference between values in columns 6 and 11 (%)
13. Difference between values in columns 7 and 11 (%)
14. Difference between values in columns 8 and 11 (%)
15. Difference between crack extension computed using range counting and rainflow for segment A (%)

Notes:

1. Values in columns 12, 13, 14 show difference between real and rainflow counted crack extension
2. Negative values in column 15 indicate unconservative nature of computations from range counting
3. Stepwise variation in peak/trough level in A, B is given by: step = $(1000 - L^*)/n$
4. Range of counted interruptions is given by: range = $L^* - L_{min}$ − step

FIG 35 SEVEN DIFFERENT LOAD SEQUENCES USED IN TESTS AND EQUIVALENT STRIATION PATTERN ALONG WITH TABLE OF RESULTS OF FRACTOGRAPHIC ANALYSIS.

by-flight combat aircraft spectrum loading with the objective of evaluating the effect of dK/da in a specific manner (Sunder 1984). Fatigue crack growth tests were carried out on single edge cracked specimen, under flight simulation combat aircraft spectrum loading under constant mean stress levels of S_m=15, 20 and 25 MPa fatigue crack growth tests were also carried out under K-control simulating linear variation of mean stress intensity K_m with a zero, positive and negative K_m gradients were simulated in the test.

Fig.36 shows the K_m functions simulated in the tests and also crack growth rates plotted against K_m for all test results obtained. The lack of correlation between K_m and growth rates is evident. The results in Fig.37 show the dependence of growth rates on dK_m/da and the mean stress levels. An explanation for the dependence of growth rates on dK_m/da is proposed on the basis of crack closure. de Koning and Van der Linden (1981) showed that crack opening stress level is determined by a competition of residual deformations in the wake and ahead of the crack tip. A large plastic zone ahead of the crack tip will keep the crack open even at zero load if the wake is not sizable. On the other hand, a large wake with a small plastic zone ahead of the crack tip will create a 'hump' effect and close the crack at a higher load level. It follows that residual deformations in the wake of the crack tip contribute to increase in crack closure stress while those ahead of the crack tip tend to reduce crack closure stress. Fig.38 shows schematically the deformations in the wake and ahead of the crack for $dK/da = 0$ > 0 and < 0 conditions. It is evident that $dK/da < 0$ conditions result in a higher crack joining stress level than $dK/da > 0$ conditions. It should be observed that in spectrum loading, the crack opening stress level is controlled by the truncation level in the spectrum or the maximum stress level in the spectrum. In the test results reported, the truncation level is nine 'g'. Hence the K gradient for the nine 'g' stress level will be nine times of the K_m gradient. This large gradient in K at max stress level in the spectrum can affect the crack opening stress level significantly. Even though the change in crack opening stress level may not be significant in magnitude with respect to the maximum stress level, it could be very significant compared to the lower stress levels in the spectrum. Since the maximum contribution to crack growth is made by the intermediate stress level in the spectrum, the effects of dK_m/da show up prominantly. Fig.39 shows the measured crack opening stress level for different K-function loadings.

An important observation that can be made from this study is that any laboratory data obtained under flight simulation fatigue crack growth testing cannot be easily used to predict fatigue crack growth in structures due to lack of correlation with characteristic K (or K_m) and the effect

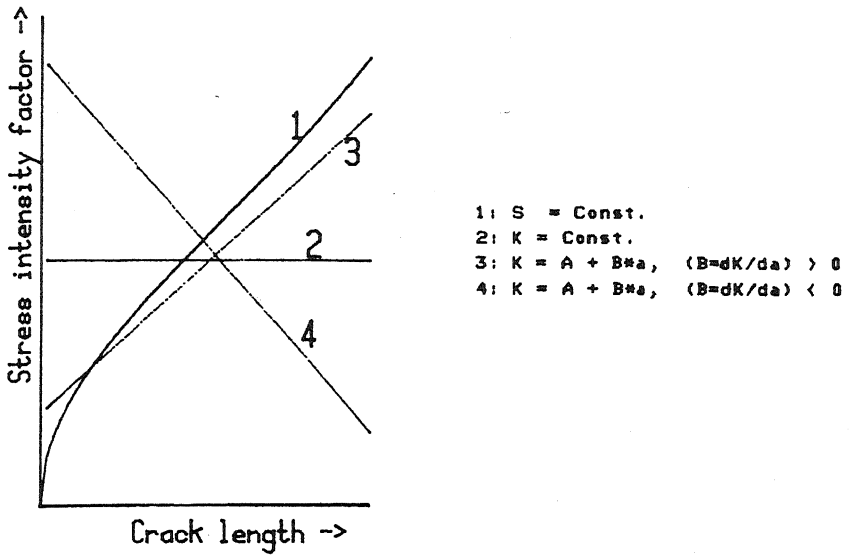

FIG 36 K_m - FUNCTIONS SIMULATED IN TESTS

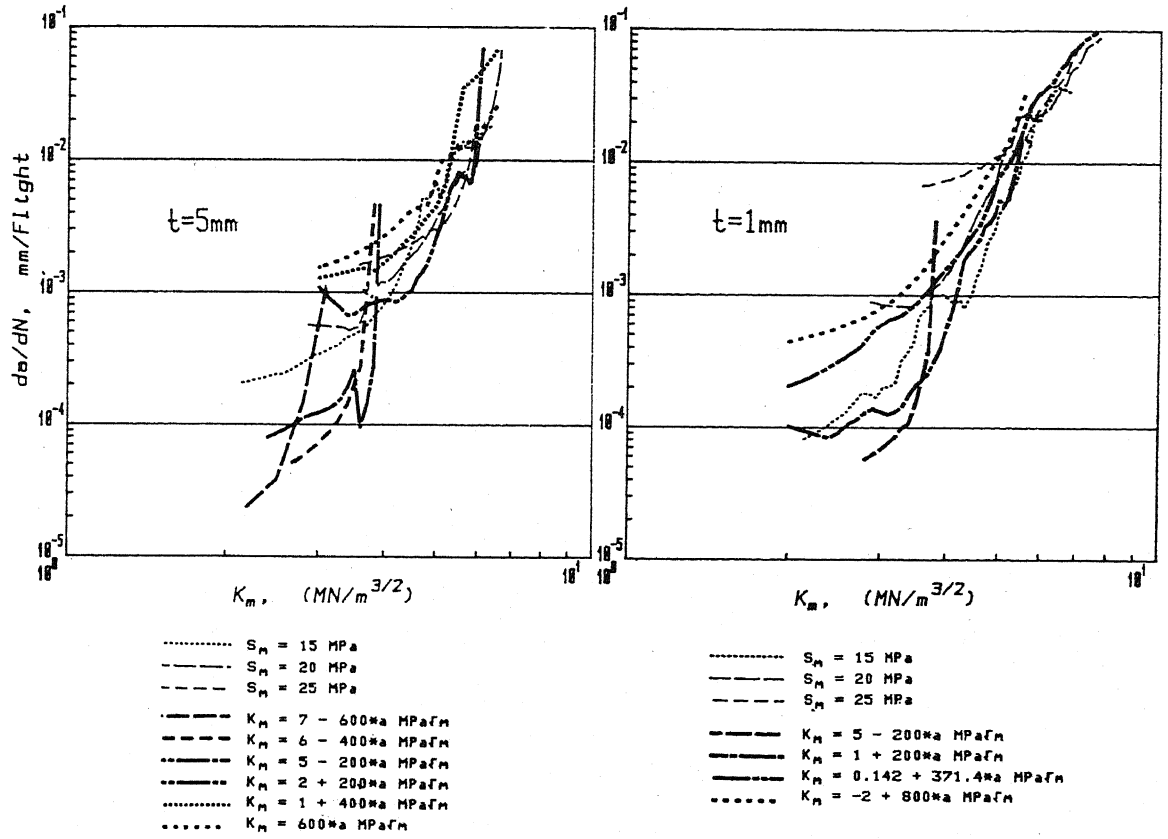

FIG 37 CRACK GROWTH RATE Vs K_m PLOTS OBTAINED FROM TESTS UNDER DIFFERENT LEVELS OF MEAN STRESS AND dK/da

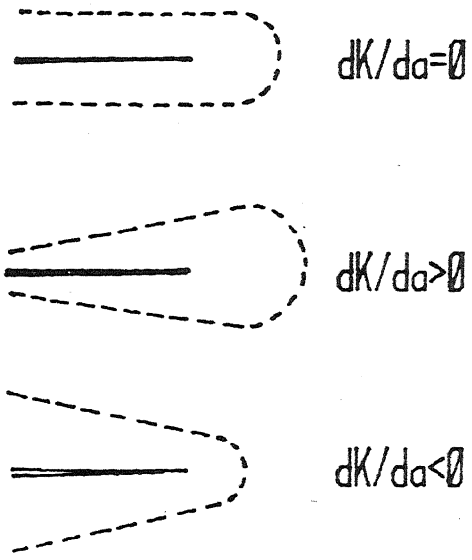

FIG 38 RESIDUAL CRACK TIP DEFORMATIONS FOR DIFFERENT K - GRADIENT TEST CONDITIONS.

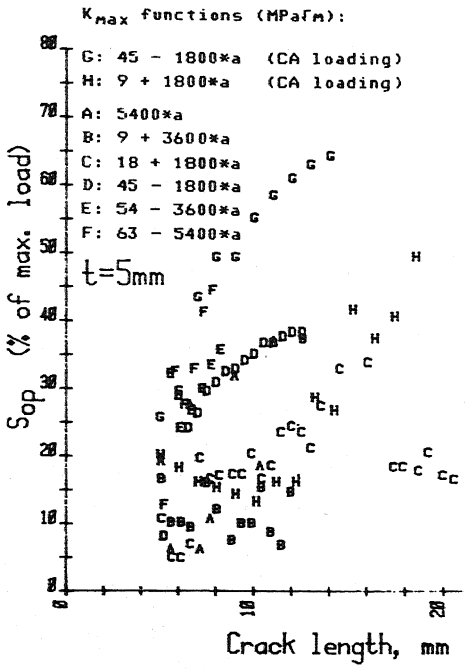

FIG 39 MEASURED CRACK OPENING STRESS LEVELS UNDER CONSTANT AMPLITUDE AND SPECTRUM LOADING CONDITIONS.

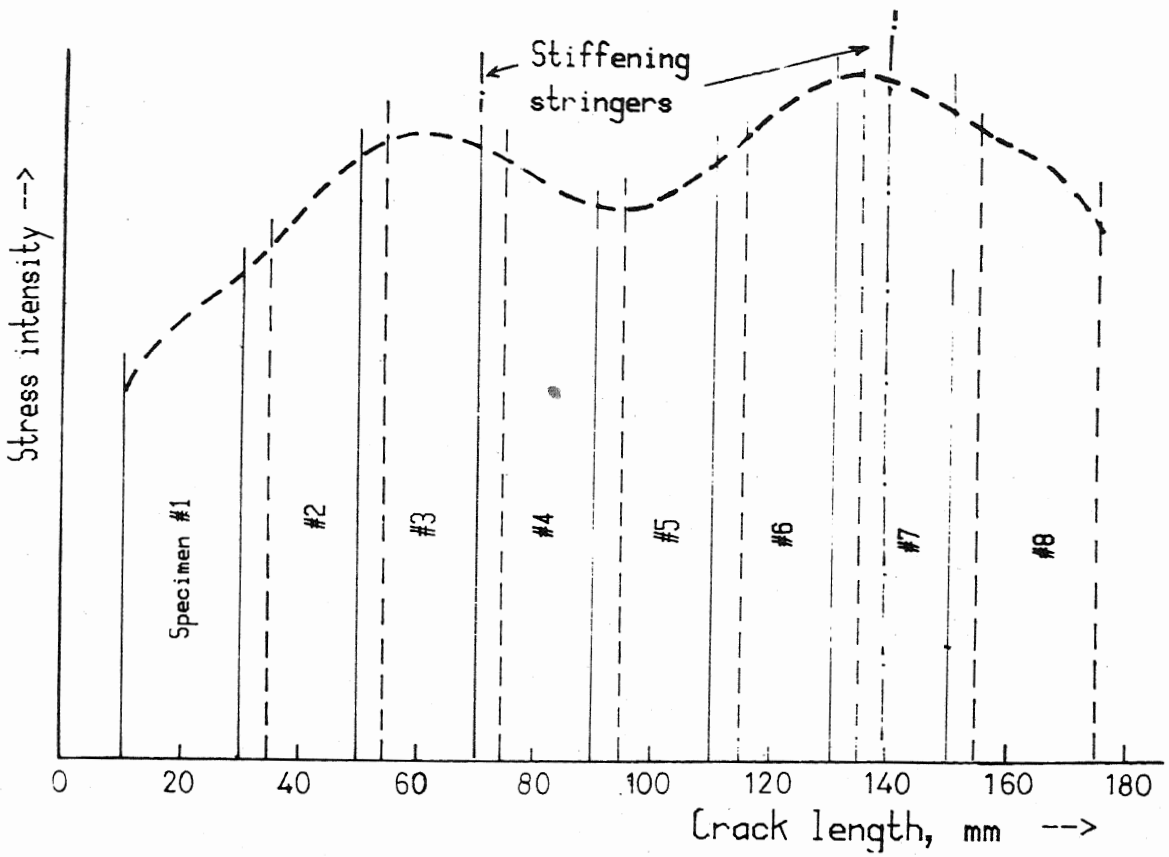

FIG 40 SEGMENT SIMULATION TECHNIQUE (SST) - SEGMENT SIMULATION OF K - FUNCTION OF STIFFENED PANEL - VERTICAL LINES DEMARCATE SEGMENTS TO BE SIMULATED ON INDIVIDUAL SPECIMEN: DOTTED LINES INDICATE OVERLAP

of dK/da. An engineering solution to this problem is to use the so called segment simulation technique (SST). Let a wing skin panel for which fatigue crack growth prediction is required for flight loading, have a K function of the type shown in Fig.40. The K function can be broken into multiple segments, each covering a crack length interval well within the width of a standard laboratory SENT (Single Edge Notched Tension) specimen as indicated in the figure.

As per SST, using eight 75 mm wide SENT specimens, one can simulate crack propagations in a panel with crack growth interval exceeding 170 mm. Each specimen would cover a segment of 25 to 30 mm only. Both K and dK/da over this interval in the specimen should coincide with those in the corresponding panel segment. The K function for segments to be simulated in individual specimens can be adequately approximated by a fourth order polynomial. Test data under flight simulation loading obtained on these specimens can then be put together to predict crack growth in the panel.

B.4 PHOTOELASTIC DETERMINATION OF STRESS INTENSITY FACTORS FOR CFRP PATCHED EDGE CRACKED PLATES

(Subramanyam and Co-workers 1983)

Photoelastic investigations have been carried out to determine the effect of CFRP patches on stress intensity factors for edge cracked plates in tension. The parameters investigated are the length and location of CFRP patches. Fig.41 indicates the isochromatic fringe patterns obtained in a photoelastic edge cracked specimen with a CFRP patch. Characterisation of fracture resistance of CFRP patched single edge cracked Al-alloy specimen by J integral evaluated experimentally using strain gage technique has also been attempted.

B.5 FATIGUE CRACK GROWTH IN CFRP PATCHED PLATES UNDER CONSTANT AMPLITUDE AND FLIGHT SIMULATION LOADINGS

(Rameshchandra and Sunder 1984)

Fatigue crack growth was studied in aluminium alloy plates reinforced by adhesive bonding a unidirectional carbon fibre epoxy patch across the crack path. Tests were carried out under constant amplitude and flight-by-flight combat aircraft spectrum loading. Comparative tests were also conducted on unpatched plates. The composite patch considerably reduces crack growth rates. The improvement in resistance to fatigue crack growth is more pronounced under spectrum loading condition. Fig.42 shows crack growth rates as a function of crack length for patched and unpatched conditions under constant amplitude and spectrum loading at 1 'g' stress levels of 80 MPa and 25 MPa respectively.

CONCLUDING REMARKS

R&D activity at NAL in the area of fatigue and fracture ranges from basic studies on materials behaviour to work of applied nature involving fatigue testing of large scale structures such as airframes. An important segment of the activities is the design, fabrication and setting up of sophisticated testing facilities in addition to developing new techniques of fatigue crack growth testing under complex loadings which merits to be considered as front line work in testing technology.

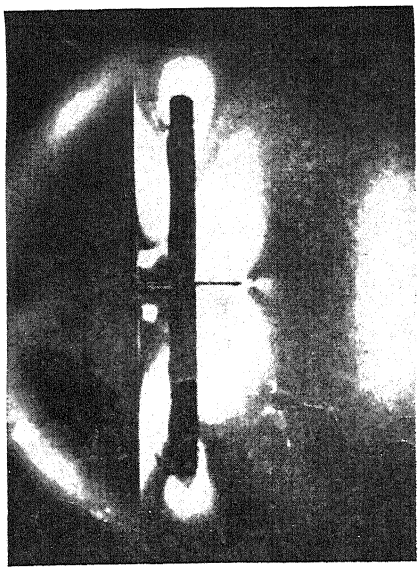

FIG 41 PHOTOELASTIC SEN SPECIMEN WITH A PATCH SHOWING ISO-CHROMATIC FRINGES

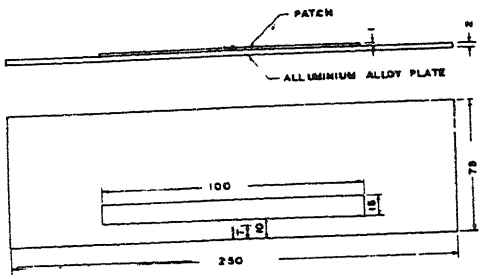

GEOMETRY OF SPECIMEN

CONSTANT AMPLITUDE da/dN

S = 80 MPa.

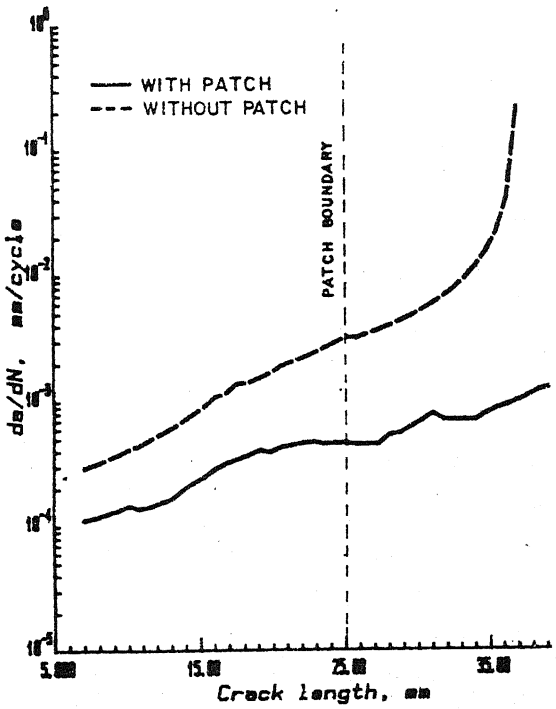

SPECTRUM LOADING da/dN

S_m = 25 MPa

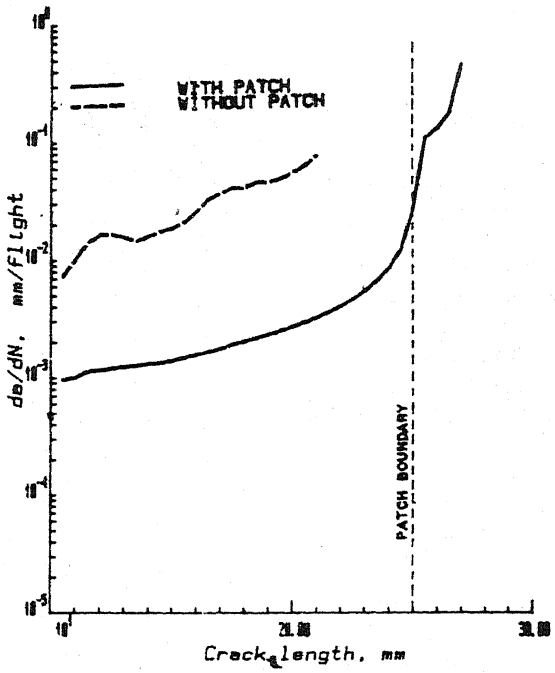

FIG 42 FATIGUE CRACK GROWTH RATES IN PATCHED SPECIMEN UNDER CONSTANT AMPLITUDE AND FLIGHT SIMULATION LOADING

Some of the research work such as the fractographic technique of crack opening stress determination, fractographic validation of cycle counting technique, fatigue crack growth under flight simulationn loading with K-control and the analytical modelling of fatigue crack growth in an unified manner based on energy balance, are bound to have a significant impact on the progress in the field of fatigue and fracture mechaniçs.

The life evaluation programmes have contributed very useful results to the IAF and HAL.

Future programmes of work include, application of fractographic event registration technique to study growth of short part through cracks initiated at notches, studies on CFRP composites under flight simulation loading at laminate level, joints level and structural component level, studies to determine threshold levels under spectrum loading conditions, and further developments in segment simulation techniques.

ACKNOWLEDGEMENT

The work described in the paper carried out over a period of more than a decade would not have been possible but for the encouragement and guidance of Dr. Valluri.

REFERENCES

Antolovich, S.D., Saxena, A., and Chanani, G.R. (1975). Eng. Fract. Mech.,7, 649-652.

Badaliance, R. (1980). Eng. Fract. Mech., 13, 657-666.

Balakrishna, S., (1976) NAL TM-IN-211, NAL, Bangalore

Barsom, J.M. (1971). In ASTM STP 486. ASTM, Philadelphia

Barsom, J.M. (1971). Trans. ASME, J. Eng. Ind., 6, 1190.

Barsom, J.M. (1976). In ASTM STP 595. ASTM, Philadelphia.

Bell, P.D., and Wolfman, A. (1976). In ASTM STP 595. ASTM, Philadelphia.

Broberg, K.B. (1975) J. Mech. & Physics of Solids, 23, 215-237.

Chang, J.B. (1981). in ASTM STP 748. ASTM, Philadelphia.

Cherepanov, G.P., and Halmonov, H. (1972). Eng. Fract. Mech., 4, 219 - 230.

Christensen, R.H., (1959), Fatigue Cracking, Fatigue damage and their detection, New York.

Cioclov, D.D. (1977). In Fracture 77 - Proc. ICF 4, Waterloo

Collipriest, J.E. (1972). North American Rockwell Report SD72-CE-12.

Dash, P.K. (1983) NAL TM-MT108/1-83, NAL, Bangalore

de Jonge, J.B. (1982). NLR Report MP 82039U, NLR, Amsterdam

de Koning, A.U. (1980). NLR Report MP 80006U. NLR, Amesterdam.

de Koning, A.U and van der Linden, H.H. (1981). Proc. 11th ICAF Symp. NLR Netherlands.

Donahue, R.J., Clark, H.M., Atanmo, P., Kumble, R.G., and McEvily, A.J. (1972) Int. J. Fract. Mech., 8, 209.

Duggam, T.V. (1977), Eng. Fract. Mech., 9, 735-747.

Duggan, T.V. and Chandler, D.C. (1979). In Mechanical Behaviour of Materials. JSME, Kyoto.

Elber, W. (1970), Eng. Fract. Mech., 2, 37-45.

Elber, W. (1971), In ASTM STP 486, ASTM, Philadelphia

Fleck, W.G., and Anderson, R.B. (1969). In Fracture 69 - Proc. 2nd Int. Conf. Fract., Brighton.

Forman, R.G., Kearney, V.E., and Engle, P.M. (1967). ASME Trans., J. Basic Engg., D-89.

Frost, N.E., and Dixon, J.R. (1967). Int. J. Fract. Mech., 3, 301-316.

Gallina, V., Galotto, C.P., and Omini, M. (1967). Int. J. Fract. Mech., 3, 37.
Grosskreutz, J.C. (1971). In ASTM STP 495, ASTM, Philadelphia.
Hartranft, R.J. and Sih, G.C., (1968) J. Maths and Physics 47, 276-291.
Havner, K.S. and Glassco, J.B., (1966), Int. J. Fract. 2, 506-525.
Head, A.K. (1953), Phil. Mag., 4, 925.
Heald, P.T., Lindley, T.C., and Richards, C.E. (1972). Mat. Sci. Eng., 10.
Hoeppner, D.W., and Krupp, W.E. (1974). Eng. Frac. Mech., 6, 47-70.
Hsu, T.M., and Lassiter, L.W. (1974). AIAA Paper No. 74-365.
Hudson, G.M., and Hardrath, H.F. (1961). NASA TND 960. NASA, Langley.
Hudson, C.M., and Raju, K.N. (1970). NASA TN-D-5702. NASA, Langley.
Ikeda, S., Izumi, Y., and Fine, M.E. (1977). Eng. Fract. Mech., 9.
Izumi, Y., and Fine, M.E. (1979). Eng. Fract. Mech., 11.
Jategaonkar, R.V., Subbarao, V.N. and Balakrishna, S. (1976). NAL TM-IN-211, NAL, Bangalore.
Johnson, W.S., Rister, W.C., and Spamer, T. (1978). ASME Trans. J. Eng. Mat. and Tech., 100, No.1, 57-63.
Johnson, W.S. (1981). In ASTM STP 748. ASTM, Philadelphia.
Jonas, O., and Wei, R.P. (1971). Int. J. Fract. Mech., 7, 116-118.
Kanninen, M.F., Atkinson, C., and McEvily, A.J. (1977). Int. J. Fract., 13, 887.
Keays, R.H. (1972). ARL Report ARL/SM 736. Melbourne.
Kocanda, S. (1978). In Fatigue Failure of Metals. Sijthoff & Noordhoff.
Krafft, J.M. (1964), Sp. Rep. to ASTM -FTHSN.
Krafft, J.M. (1965). Trans ASM, 58, 691.
Kuo, A.S., and Liu, H.W. (1976). Scripta Met., 10, 723.
Laird, C., and Smith, G.C. (1962), Phil. Mag., 7, 847-857.
Lal, K.M., and Garg, S.B.L. (1977). Eng. Fract. Mech., 10, 539-552.
Landgraf, R.W., Richards, F.D. and La Pointe, N.R. (1977) Fatigue under Complex Loading, Soc.Auto.Engg, 95
Lardner, R.W. (1968). Phil. Mag., 17, 71.
Laxminarayana, H.V., Murthy, M.V.V. and Srinath, L.S., (1982) Int. J. Fract. 19, 257-275.
Liu, H.W. (1963). ASME Trans. J. Basic Eng. 116-122.
Liu, H.W., and Iino, N. (1969). In Fracture 69 - Proc. 2nd Int. Conf. Fract., Brighton.
Maddox, S.J. (1975). Int. J. Fract., 11, 3, 389-408.
Majumdar, S., and Morrow, J.D. (1974). In ASTM STP 559 ASTM, Philadelphia.
Mathews, W.T., Barrata, F.I., and Driscoll, G.W. (1971). Int. J. Fract. Mech. 7, 224-228.
Matsuishi, M. and Ehdo, T., (1968) Proceedings of Kyushu Meeting of JSME
McClintock, F.A. (1963). In Fracture of Solids. Interscience, New York.
McEvily, A.J., and Illg, W. (1959). In ASTM STP 274., ASTM, Philadelphia.
McEvily, A.J. (1974). Met. Sco. London, 204.
McEvily, A.J., Baukelmann, D. and Tanaka, K. (1976). In Strength and Structure of Solid Materials. Noordhoff.
McMillan, J.C., and Hertzberg, R.W. (1968). In ASTM STP 436. ASTM, Philadelphia.
McMillan, J.C. and Pelloux, R.M.N., (1970) Engg.Fract.Mech 2, 81-84.
Mills, W.J., and Hertzberg, R.W. (1975). Eng. Fract. Mech., 7, 705.
Mills, W.J. and Hertzberg, R.W. (1976). Eng. Fract. Mech., 8, 657.
Mura, T., and Lin, C.T. (1974). Int. J. Fract. Mech., 10.
Musuva, J.K., and Radon, J.C. (1979). DVM, Stuttgart, 479-494.
Musuva, J.K., and Radon, J.C. (1980). In Proc. 3rd Colloquium on Fracture ECF3, Pergamon.
Neumann, P. (1967). Acta Met., 17.

Neumann, P. (1974). Acta Met.
Newmann, J.C. (1981). In ASTM STP 748. ASTM, Philadelphia.
Paris, P.C., Gomez, M.P., and Anderson, W.E. (1961). The Trend in Eng., 13, Univ. of Washington.
Paris, P.C. (1969). In Fatigue - An Interdisciplinary Approach. Syracuse Univ.
Paris, P.C., Bucci, R.J., Wessel, E.T., Clark, W.G., and Mager, T.R. (1972). In ASTM STP 513. ASTM, Philadelphia.
Pearson, S. (1972). Eng. Fract. Mech., 4, 9-24.
Pearson, S. (1975). Eng. Fract. Mech., 7. 235-247.
Pelloux, R.M.N. (1970). AFFDL-TR 70-144.
Poe, C.C. (1971). In ASTM STP 486. ASTM, Philadelphia.
Potter, J.M. (1973). In ASTM STP 519. ASTM, Philadelphia.
Proctor, H.W., and Duggan, T.V. (1979). In Fracture Mechanics in Engineering Application, Sijthoff & Noordhoff.
Raju, K.N. (1969). Int.J.Fract 5, 101-112.
Raju, K.N., Ningaiah, S., and Rao, B.V.S. (1972). Int. J. Fract. Mech.,1. 99.
Raju, K.N. (1972). Int. J. Fract. Mech., 8, 1-14.
Raju, K.N. (1973-82). Progress reports on full scale fatigue testing programmes.
Raju, K.N. (1980). PhD Thesis. Indian Institute of Science, Bangalore.
Sunder, R., and Raju, K.N. (1982). NAL TM-MT-7-82 NAL, Bangalore.
Raju, K.N. (1983). NAL-TM-MT-103/1-83. NAL, Bangalore.
Raju, K.N., and Sunder, R. (1984). NAL TM-MT-7-84, NAL, Bangalore and also ICF6 Plenary Paper.
Ramesh Chandra and Sunder, R. (1984). ICF paper.
Rhodes, D., Culver, L.E., and Radon, J.C. (1981). In Proc. Fatigue '81. Westbury House, London.
Rice, J.R. (1967). In ASTM STP 415. ASTM, Philadelphia.
Richards, C.E., and Lindley, T.C. (1972). Eng. Fract. Mech. 4. 951-978.
Ritchie, R.O. (1979). Int. Metals Review, 24, 205.
Ritchie, R.O., Suresh, S., and Moss, C.M. (1980). Trans. ASME. J. Eng. Mat. Tech., 102. 293-299.
Saxena, A., and Hudak, S.J. Jr. (1978). Int. J. Fract., 14, 453-463.
Schijve, J. (1960). NLR Report MP195. NLR, Amsterdam.
Schijve. J., Broek, D., and de Rijk, P. (1961). NLR-TN M2094,Nlr, Amsterdam.
Schijve, J., Jacobs, F.A., and Tromp, P.J. (1968). NLR TR 68117. NLR, Amsterdam.
Schijve, J., Jacobs, F.A., and Tromp, P.J. (1972). NLR TR 72018. NLR, Amsterdam.
Schijve, J. (1973). Eng. Fract. Mech., 5. 269-280.
Schijve, J. (1974). Eng. Fract. Mech., 6. 245-252.
Schijve, J. (1976). In ASTM STP 595. ASTM, Philadelphia.
Schijve, J. (1980). In ASTM STP 700. ASTM, Philadelphia.
Schijve, J.. (1980). Memorandum M-358. Delft University, DELFT.
Schwalbe, K.H. (1973). Int. J. Fract., 9. 381-395.
Schwalbe, K.H. (1974). Eng. Fract. Mech., 6. 325-341.
Schwalbe, K.H. (1979). Eng. Fract. Mech., 11. 331-342.
Sih, G.C., and Berthelemy, B.M. (1980). Int J. Fract. Mech., 13, 439-451.
Stephens, R.I. (1977). In ICAF Doc. No.960. Darmstadt.
Stouffer, D.C., and Williams, J.F. (1979). Eng. Fract. Mech., 11. 525-536.
Subramanyam, A., Rameshchandra, Murthy, M.V.V. and Rao, A.K., (1981) Engg. Fract.Mech 18,2, 305-313
Sunder, R. (1978). PhD Thesis. Kiev Institute of Civil Aviation, Kiev.
Sunder, R. (1979a). Eng. Fract. Mech., 12. 147-154.

Sunder, R. (1979b). Eng. Fract. Mech., 12. 155-165.
Sunder, R., and Dash, P.K. (1982). Int. J. Fatigue. April, 97-105.
Sunder, R. (1982). NAL-TM-MT-8-82. NAL, Bangalore.
Sunder, R. (1982). NAL-TM-MT-9-82. NAL,Bangalore.
Sunder, R., and Raju, K.N. (1982). NAL-TM-MT-7-82. NAL, Bangalore.
Sunder, R. (1983). NAL-MT-TM-10-83. NAL, Bangalore.
Sunder, R., Seetharam, S.A. and Bhaskaran, T.A. (1983). NAL-TM-MT-7-83 NAL, Bangalore, also in (1984) Int. J. Fatigue, 6,3. 147-156.
Sunder, R. (1984). NAl-TM-MT-2-84. NAL, Bangalore.
Sunder, R. (1984). NAL-TM-MT-2-84. NAL, Bangalore, also Presented at Fatigue 84, Sept 1984.
Sunder, R. (1984). NAL-TM-MT-8-84. NAL, Bangalore.
Sunder, R. (1984). NAL-TM-MT-9-84. NAl, Bangalore.
Suresh, S. (1982). Report LBL-14482. University of California.
Tomkins, B. (1968). Phil. Mag., 18. 1041-1066.
Tomkins, B. (1969). J. Eng. Mat. and Tech. Trans. ASME Ser. H., 97. 289-297.
Topper, T.H., and El. Haddad, M.H. (1982). In Fatigue Thresholds Vol.2. EMAS, Warley.
Valluri, S.R. (1961). Aerosp. Eng., 20. 18-19 and 68-69.
Valluri, S.R., Glassco, J.B., and Bockrath, G.E. (1963). Douglas Aircraft Report No. EP 1695.
Valluri, S.R. (1965). Proceedings of First International Conf on Fract, Sendai 3. 1727-1738.
Vogelesang, L.B. (1975). In ICAF DOC 80. 2.2/01-29.
von Euw, Hertzberg, R.W., and Roberts, R. (1972). In ASTM STP 513. ASTM, Philadelphia.
Wanhill, R.J.H. (1978). NLR MP 78015. NLR, Amsterdam.
Weertman, J. (1969). Int. J. Fract. Mech., 5. 13-15.
Weertman, J. (1973). Int. J. Fract., 9. 125-131.
Weertman, J. (1978). In Fracture Mechanics. Univ. Press of Virginia, Charlottesville.
Weiss, V. (1964). In Fatigue - An Interdisciplinry approach. Syracuse University, Syracuse.
Wheeler, O.E. (1972). ASME Trans Series D.J. Basic. Eng..
Willenborg, J.D., Engle, R.M., and Wood, H.A. (1971). AFFDL-TM-FBR-71-1.
Wnuk, M.P. (1971). Int. J. Fract. Mech., 7. 383-407.
Wnuk, M.P. (1973). Eng. Fract. Mech., 5. 379-398.
Yokobori, T., and Ichikawa, M. (1968). Rep. Res. Inst. Str. and Fract. Mat., Tohoku Univ., 4, 45-53.
Yokobori, T., Kawagishi, M., and Yoshimura, T. (1969). In Fracture 69 - Proc. 2nd Int. Conf. Fract., Brighton.